TECHNICAL REPORT BRL-TR-3288

BRL

PYROLYSIS GC-FTIR STUDIES OF A LOVA PROPELLANT FORMULATION SERIES: FINAL REPORT

ROSE A. PESCE-RODRIGUEZ
FREDERICK J. SHAW
ROBERT A. FIFER

NOVEMBER 1991

U.S. ARMY LABORATORY COMMAND

BALLISTIC RESEARCH LABORATORY
ABERDEEN PROVING GROUND, MARYLAND

NOTICES

Destroy this report when it is no longer needed. DO NOT return it to the originator.

Additional copies of this report may be obtained from the National Technical Information Service, U.S. Department of Commerce, 5285 Port Royal Road, Springfield, VA 22161.

The findings of this report are not to be construed as an official Department of the Army position, unless so designated by other authorized documents.

The use of trade names or manufacturers' names in this report does not constitute indorsement of any commercial product.

REPORT DOCUMENTATION PAGE

Form Approved
OMB No. 0704-0188

1. AGENCY USE ONLY (Leave blank)	2. REPORT DATE	3. REPORT TYPE AND DATES COVERED
	November 1991	Final, Nov 89 - Nov 90

4. TITLE AND SUBTITLE

Pyrolysis GC-FTIR Studies of a LOVA Propellant Formulation Series: Final Report

5. FUNDING NUMBERS

PR: F11ZFK53M1AJ

6. AUTHOR(S)

Rose A. Pesce-Rodriguez, Frederick J. Shaw, and Robert A. Fifer

7. PERFORMING ORGANIZATION NAME(S) AND ADDRESS(ES)

8. PERFORMING ORGANIZATION REPORT NUMBER

9. SPONSORING/MONITORING AGENCY NAME(S) AND ADDRESS(ES)

U.S. Army Ballistic Research Laboratory
ATTN: SLCBR-DD-T
Aberdeen Proving Ground, MD 21005-5066

10. SPONSORING/MONITORING AGENCY REPORT NUMBER

BRL-TR-3288

11. SUPPLEMENTARY NOTES

12a. DISTRIBUTION/AVAILABILITY STATEMENT

Approved for public release; distribution is unlimited.

12b. DISTRIBUTION CODE

13. ABSTRACT (Maximum 200 words)

Pyrolysis-gas chromatography-Fourier transform infrared (P-GC-FTIR) spectroscopy has been used to examine the pyrolysis product distribution for a LOVA propellant formulation series. The series was provided by the Naval Weapons Center (NWC), China Lake, and contained the oxidizers HMX and RDX, the polymers GAP, HTPB, BAMO/AMMO, and BAMO/THF, and the plasticizers BTTN and TMETN. Trends in product distribution as a function of formulation, as well as correlations between pyrolysis products and NWC performance data, were identified. The most noteworthy correlation observed was between the amount of permanent gas produced and go/no-go ignition times. In general, pyrolysis product distributions were found to be most strongly affected by the presence and type of plasticizer. The results of this investigation may serve as a basis for formulation design and bench-scale propellant screening.

14. SUBJECT TERMS

Pyrolysis products; Pyrolysis-GC-FTIR; LOVA propellants; PBX propellants; gas chromatography; pyrolysis

15. NUMBER OF PAGES
56

16. PRICE CODE

17. SECURITY CLASSIFICATION OF REPORT	18. SECURITY CLASSIFICATION OF THIS PAGE	19. SECURITY CLASSIFICATION OF ABSTRACT	20. LIMITATION OF ABSTRACT
UNCLASSIFIED	UNCLASSIFIED	UNCLASSIFIED	UL

INTENTIONALLY LEFT BLANK.

TABLE OF CONTENTS

INTENTIONALLY LEFT BLANK.

LIST OF FIGURES

INTENTIONALLY LEFT BLANK.

LIST OF TABLES

INTENTIONALLY LEFT BLANK.

ACKNOWLEDGMENT

We thank Dr. Rena Y. Yee of the Naval Weapons Center, China Lake, CA, for providing samples and performance test results used in this study.

INTENTIONALLY LEFT BLANK.

1. INTRODUCTION

A considerable amount of information has been published concerning the mechanisms and products of the thermal decomposition of the nitramines cyclotrimethylene trinitramine (RDX) and cyclotetramethylene tetranitramine (HMX). Fifer (1984) and Schroeder (1985, 1988) are useful reviews of the literature. Until recently, these studies primarily involved measurement only of the permanent gases (CO_2, NO_2, NO, CH_2O, HCN, N_2O, N_2, etc.) in the products, or involved mass spectral studies under vacuum conditions where it is difficult to distinguish pyrolysis from ionization-induced fragmentation of vaporized nitramine molecules. During the last several years, two developments have led to the identification of larger fragments in the pyrolysis products. One is the application of fused silica capillary column gas chromatography (GC) techniques (Fifer et al. 1986; Schroeder 1987). The other involves new mass spectral techniques involving time-of-flight measurements to determine the parent peak leading to each ion fragment (Behrens 1987; Zhoa, Hintsa, and Lee 1988) or employing atmospheric pressure chemical ionization and tandem mass spectrometric techniques to minimize vaporization and provide information on the structures of observed product masses (Snyder et al. 1990).

The majority of the published studies have concentrated on the development of mechanisms to explain the formation of the observed decomposition products. There have been very few attempts to correlate pyrolysis product distributions with large-scale performance tests such as ignitability, impact sensitivity, or burn rate. Since definitive mechanistic information has not been forthcoming for the nitramines and nitramine propellants, the search for correlations may be a more fruitful approach. Mechanisms are not required, only a correlation of one or more features in the pyrolysis product distributions with the performance property of interest. Once such a correlation is found, the pyrolysis measurement becomes a small-scale screening test for the desired performance property, one that perhaps does not require fabrication on a large scale, or that might require only unprocessed mixtures of potential ingredients. Also, the correlation may suggest rules that can be used in expert systems for computer assisted formulations design and properties prediction (Morris and Fifer 1990). Correlating pyrolysis product distributions with performance is analogous to reported correlations between Low Vulnerability Ammunitions (LOVA) propellant sensitivity with binder/acid DSC decomposition temperature (Wise and Rocchio 1981; Salo 1988). The information content in a product distribution measurement, where

perhaps 15 or 20 products are measured, is much greater than in a thermokinetic measurement where only a single property (e.g., decomposition temperature) is measured, so there should be an even greater likelihood of finding a useable correlation.

The principle reason why pyrolysis-performance correlations have not been attempted is that a suitable series of systematically varied propellant formulations, with properly documented performance measurements, has not been available. Such a LOVA formulation series has been developed at the Naval Weapons Center (NWC), China Lake, CA, by Dr. Rena Yee (1985; 1988; 1987) who provided both samples and performance test data for this study. In the formulation series, oxidizer and binder were systematically varied. Performance test results include burn rate, impact sensitivity, and time-to-ignition for radiative heating (CO_2 laser, 10.6 μm). This formulation series contains either RDX or HMX as the oxidizer and one of the following polymers: hydroxy-terminated polybutadiene (HTPB), glycidyl azide polymer (GAP), 3,3-bis-azidomethyl oxetane/tetrahydrofuran (BAMO/THF) copolymer, or 3,3-bis-azidomethyl oxetane/3,3-bis-azidomethyl-3-methyl oxetane (BAMO/AMMO) copolymer. The azido polymers were plasticized with either trimethylolethane trinitrate (TMETN) or 1,2,4-butane trinitrate (BTTN). The composition of each formulation is given in Table 1. Samples of HMX, RDX, GAP, HTPB, and plasticizers were also analyzed.

Although the initial purpose of this investigation was to identify correlations between pyrolysis product distributions and ignition times (Shaw and Fifer 1988), several other trends related to propellant formulation were observed and will also be discussed in this report. The sample set provided the opportunity to observe not only the correlations of pyrolysis product distribution with radiative ignition time, but also the effect of formulation on pyrolysis product distribution. It is hoped that the results of this investigation will be useful to those interested in propellent design and performance prediction.

2. EXPERIMENTAL

All samples were pyrolyzed using a Chemical Data Systems (CDS) Model 122 Pyroprobe connected via a heated interface chamber to the injector of a Hewlett-Packard 5965 GC-FTIR equipped with a capillary column and liquid nitrogen cooled Mercury Cadmium Telluride (MCT) detector (Hewlett-Packard Model 5965A infrared detector).

Table 1. Composition of Propellant Formulations (in weight-percent)

Sample	RDX	HMX	Polymer[a]	Polymer Type	Plasticizer	Plasticize Type
4	74.8	0.0	6.3	GAP	18.9	TMETN
8	68.4	0.0	31.6	GAP	0.0	–
9	65.9	0.0	11.5	GAP	22.6	BTTN
14	0.0	69.7	30.3	GAP	0.0	–
15	0.0	0.0	50.0	GAP	50.0	BTTN
16	75.0	0.0	25.0	HTPB	0.0	–
17	0.0	76.0	24.0	HTPB	0.0	–
18	0.0	0.0	50.0	GAP	50.0	TMETN
19	65.0	0.0	17.5	GAP	17.5	BTTN
20	0.0	66.3	16.8	GAP	16.9	BTTN
21	0.0	67.6	16.2	BAMO/THF	16.2	BTTN
22	0.0	68.2	15.9	BAMO/AMMO	15.9	TMETN
23	0.0	68.6	15.7	BAMO/THF	15.7	TMETN
24	0.0	68.3	15.8	GAP	15.9	TMETN
25	67.1	0.0	16.5	GAP	16.4	TMETN

[a]Includes curing agent.

The pyrolysis sample (ca. 1 mg) was placed in a quartz tube and held in place with glass wool. The tube was then inserted into a coil-type Pyroprobe. The probe was inserted into the heated interface which was continuously being swept with carrier gas. Once enough time had elapsed to allow the carrier gas to sweep all air from the interface compartment and to allow the sample to reach thermal equilibrium, the sample was flash heated to the pyrolysis temperature and held at that temperature for 20 s. The pyrolysis products then passed through the splitless injector into the capillary column, which separated the products for detection and identification. As each component eluted from the capillary column, it passed through a light pipe in the beam of an interferometer for spectroscopic analysis by Fourier transform infrared (FTIR) spectroscopy. Table 2 lists the pyrolytic, chromatographic, and spectroscopic conditions for the experiments. Figure 1 shows a schematic representation of the apparatus.

Table 2. Pyrolytic, Chromatographic, and Spectrographic Conditions

Pyroprobe and interface parameters:	
interface temperature	100° C
pyrolysis temperature	400° C, 500° C, 1,000°
heating mode	°C flash heating
heating time	20 s
sample size	ca. 1 mg
configuration	quartz sample tube in coil-type probe
GC oven/column parameters:	
initial temperature	50° C
initial hold time	3 min
heating rate	10 deg/min
final temperature	200° C
final hold time	5 min
injection port temperature	200° C
light pipe temperature	250° C
transfer line temperature	250° C
column	0.32 mm x 25 m OV-17, 3-μm film Quadrex Corp.
FTIR parameters:	
detector	MCT, narrow band
resolution	3 cm^{-1}
scan rate	3 scans/s

Each of the samples was pyrolyzed at both a low and high temperature. For the low temperature experiments, RDX formulations and formulations of GAP/plasticizer (samples 15 and 18) were pyrolyzed at 400° C, while HMX formulations were pyrolyzed at 500° C. For the high temperature experiments, all samples were pyrolyzed at 1,000° C. Low temperature experiments were not carried out for GAP and HTPB because of their thermal stability. Thermocouple measurements indicated that the actual temperatures experienced by samples in the quartz tubes were 150–200° C lower than the pyroprobe set temperatures. The low temperature experiments were, therefore, just above the melting points of RDX and HMX (204° C and 280° C, respectively). Three experiments were carried out for each of the samples at each of the two temperatures to insure reproducibility.

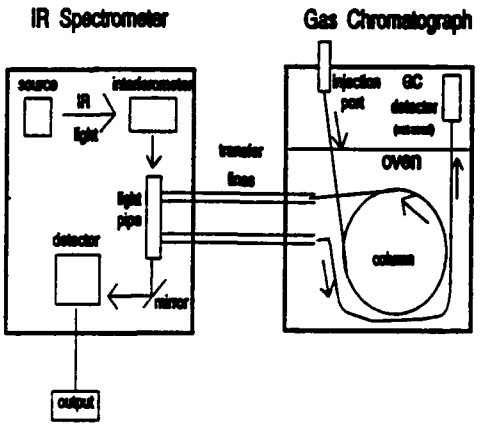

Figure 1. Schematic Representation of GC-FTIR Apparatus.

Gas chromatograms were generated by application of the Gram-Schmidt algorithm to the FTIR detector output (Griffiths and Haseth 1986). Peaks were then identified by examination of the associated FTIR spectra. A small fraction of the peaks was directly identified by an automated search of the Environmental Protection Agency (EPA) library of vapor phase spectra. Software for this search was provided by the manufacturer.

Retention times were corrected to give the permanent gas peak at 0.0 min. Quantification of pyrolysis products was based on GC peak areas and is reported in area percent in Tables 3, 4, 5, and 6. Exceptions to this are the individual permanent gas products which are not readily quantified by GC peak area because they elute within a few seconds of each other and appear as a single GC peak. For this reason, individual permanent gas quantities were calculated from FTIR absorbance and are given in normalized absorbance units (Tables 7 and 8). To calculate these normalized absorbance values, all FTIR spectra under the permanent gas GC peak were first summed to yield a single spectrum. The absorbance of the largest band for each permanent gas in this spectrum was then divided by the sum of the absorbances of the largest band for each gas. The bands chosen for each gas are given as follows: CH_4, 3,016 cm^{-1}; CH_2O, 2,084 cm^{-1}; CO_2, 2,363 cm^{-1}; N_2O, 2,238 cm^{-1}; CO, 2,111 cm^{-1}; and NO, 1,912 cm^{-1}. A typical permanent gas FTIR spectrum is given in Figure 2.

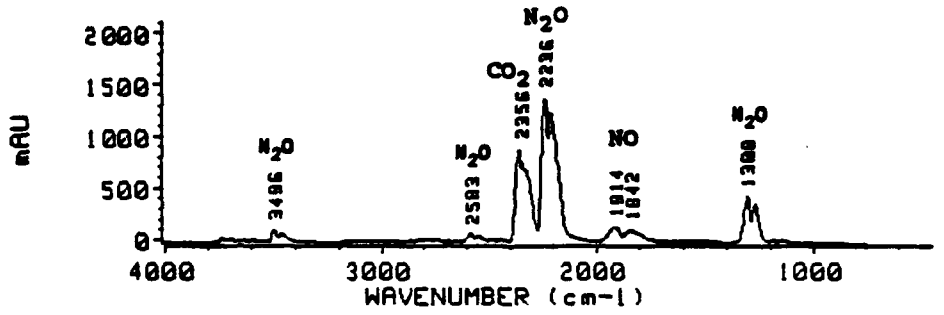

Figure 2. Typical FTIR Spectrum of Permanent Gas Pyrolysis Products.

It must be stressed that all reported values are uncalibrated, relative quantities that are only used to identify variations in pyrolysis product distributions. Magnitudes of absorbance, as well as GC peak areas, for different compounds are not comparable due to differences in infrared absorption coefficients.

Although the data reported here represent one of the most comprehensive investigations of pyrolysis product distribution for propellant formulations to date, several products are notably absent. Most of these products reacted before reaching the light pipe, and, therefore, could not be detected. These include highly reactive species such as NO_2, radicals, and ions. Other species such as N_2 and H_2 do not absorb in the infrared region, and, therefore, were not detected. In spite of this drawback, pyrolysis GC-FTIR is superior to the more commonly used GC-MS methods, with which no analysis of the permanent gases would be possible with normal unit mass resolution (unless multiple column techniques were used to permit separation of the permanent gases, as well as the larger fragments). The reason for this is that there are a number of unfortunate coincidences in the ion fragment patterns for many of the commonly observed permanent gases. For example, m/z 28 could be CO or N_2, m/z 30 could be CH_2O or NO, m/z 44 could be N_2O or CO_2, etc. With GC-FTIR this is not a problem; most of the gases have more than one absorption band, and for each gas there is at least one IR band for which there is no interference from other species.

3. RESULTS

3.1 Pyrolysis Product Distributions. The primary experimental data obtained from these experiments are GC peak areas. Retention times and FTIR spectra aid in the identification of pyrolysis products. A typical GC chromatogram and accompanying FTIR spectrum for one of the peaks in the chromatogram are given in Figures 3 and 4, respectively. Based on such information, product distributions for 15 different propellant formulations and 4 of the pure components (RDX, HMX, GAP, and HTPB) have been determined. Pyrolysis products have been divided into several catagories, i.e., permanent gases (CO_2, N_2O, CO, NO, CH_2O, CH_4), HCN, water, carbonyl compounds (amides, ketones, aldehydes, designated simply as "C=O"), carboxylic acids (RCOOH), nitrates (RNO_3), nitro compounds (RNO_2), and isocyanates (HNCO, RNCO). Permanent gases and other molecules such as acetone, acrolein, acetaldehyde, acetic acid, formic acid, and triazine were identified from their FTIR spectra. Other less readily identifiable products are classified in this report by their functionalities. Tables 3 and 4 summarize the P-GC-FTIR results for low and high temperature experiments, respectively. The tables are arranged with formulation numbers across the top of the tables and retention times down the sides of the tables. To simplify the table, retention times have been rounded off to the nearest 0.5 min. Values appearing beside each product indicate the associated GC percent-peak area.

By far, the most abundant pyrolysis products for all formulations are the permanent gases. The remainder of the products are generated by most or some of the formulations. These products are carbonyl compounds, triazine, nitro compounds, nitrates, and isocyanates. Triazine results from incomplete pyrolysis of oxidizer (HMX and RDX). Nitrates are derived from the energetic plasticizers (BTTN and TMETN). Isocyanates, other than HNCO, are likely generated from the curing agents isopherone diisocyanate and N-100, which are used to cross-link HTPB and GAP, respectively.

Pyrolysis experiments were run at two different temperatures, 400/500° C and 1,000° C, which hereafter will be referred to as low temperature and high temperature pyrolysis, respectively. Tables 5 and 6 summarize GC area-percent values for all low and high temperature pyrolysis products except individual permanent gas products, which are given in normalized absorbance units in Tables 7 and 8, respectively.

Table 3. Low Temperature Pyrolysis Products as Eluted on GC

Retention Time (min)	4 (%4)	8 (%8)	9 (%9)	14 (%14)	15 (%15)	16 (%16)	17 (%17)	18 (%18)
0	PG, H2O 79.8	PG, HCN 46.7	PG, H2O 81.0	PG, HCN, H2O 56.2	PG 84.4	PG, H2O 50.6	PG, HCN, H2O 69.6	PG 67.1
0.5		RNCO 4.8	RNCO 1.0					
1			acrolein 1.5					CH3CHO 10.0
1.5		triazine 21.2						
2		CH3COOH 2.2		acrolein 1.0	acetone 2.7	triazine 16.6	acrolein 1.0	RNCO 2.2
2.5			oxadiazole 0.4	1.0	NH3 0.6			acetone 4.7
3	CH3COOH 2.6		HCOOH 0.4					
3.5		HCOOH 4.8				HCOOH 0.5		acrolein 2.4
4		C=O, C=O 21.2	nitro- 0.4		RNCO 0.4	C=O 3.0		
4.5			methane	nitro- 1.8	CH3COOH 4.0			nitro- 0.9
5				methane	HCOOH 0.6			methane
5.5	C=O 1.2		C=O 1.0	C=O 2.5		C=O 16.7		CH3COOH 5.7
6				triazine 1.4			triazine 5.7	
6.5					RNCO 0.4	C=O 6.4		
7	RNO3 1.0				C=O 0.5	nitro- 5.6		
7.5						formamine		
8					RNCO 0.6	C=O 2.3		C=O 1.5
8.5	C=O, ., ., ., C=O 2.2		C=O 2.0		C=O, ., C=O 5.8			nitro- 1.8
9								alkane
9.5			RNCO 0.4	C=O, ., ., C=O 22.3	RNCO 0.5	C=O 0.3	C=O, ., ., C=O 18.0	
10			nitramine 6.1					
10.5	RNO3 10.3				C=O 0.2			RNCO 1.4
11	RNCO 1.6		C=O, C=O 3.1			C=O 0.1		
11.5			nitro- 0.8					
12			formamine					
12.5				other 6.7				
13							C=O 1.0	C=O 1.6
13.5								RNCO 1.6
14				nitro- 6.9			nitro- 5.1	
14.5				formamine	C=O 0.2		formamine	
15								
15.5								
16								
16.5								
17								
17.5								
18								
18.5								
19								
19.5								

19 (%19)	20 (%20)	21 %(21)	22 (%22)	23 (%23)	24 (%24)	25 (%25)	RDX (%RDX)	HMX (%HMX)	Retention Time (min)
PG 90.6	PG, HCN, H2O] 80.7	PG, HCN, H2O] 85.0	PG, HCN, H2O] 70.0	PG, HCN, H2O] 57.2	PG, HCN, H2O] 71.3	PG 82.8	PG 29.9	PG, HCN, H2O] 92.1	0
							HCOOH 4.6		0.5
							RNO3 4.2		1
							triazine 8.1		1.5
									2
C=O, ., C=O] 1.3	acrolein 1.4		acetone 1.1				C=O 7.8		2.5
							C=O 1.4		3
							C=O 0.8		3.5
					nitro-		C=O 26.9		4
			acrolein 1.4		methane 8.4	RNO3 1.6	C=O 5.2		4.5
			nitro- 0.4		CH3COOH 0.8		nitramine 1.3		5
RNO3 2.6			methane			RNO3 8.1	C=O 3.3		5.5
RNCO 2.9						RNCO	nitro- 2.5		6
RNO3 1.9						RNCO 5.7	methane	triazine 2.3	6.5
	triazine 1.4	triazine 0.3	triazine 6.9		triazine 2.5		C=O, ., ., C=O] 4.1		7
					CH3COOH 3.4				7.5
				triazine 3.2		C=O, C=O] 1.8			8
		HCOOH 2.4							8.5
	HCOOH 0.8			HCOOH 1.5	HCOOH 3.1				9
			C=O, ., ., C=O] 19.5		C=O, ., ., ., ., C=O] 8.8				9.5
									10
	C=O, ., ., C=O] 14.8	C=O, ., ., C=O] 13.3							10.5
									11
									11.5
				HCOOH 4.1				C=O 2.3	12
				HCOOH 2.9					12.5
				C=O 5.2					13
				C=O 24.3	RNO3 8.2				13.5
					C=O, ., ., ., ., ., ., C=O] 2.6				14
									14.5
									15
								C=O 3.4	15.5
									16
									16.5
				C=O 1.6					17
									17.5
									18
									18.5
									19
	C=O 1.0								19.5

Key:

PG	permanent gases	C=O	carbonyl compounds (amides, ketones, aldehydes)
RNCO	isocyanates	RNO3	nitrates
CH3COOH	acetic acid	HCOOH	formic acid
CH3CHO	acetaldehyde	HCN	hydrogen cyanide
HNCO	isocyanic acid		

] Overlapping peaks; GC peak areas have been summed.

NOTE: Pyroprobe set temperature: 400° C for RDX 500° C for HMX formulations. Retention times have been rounded off to the nearest 0.5 min. Numbers appearing to the right of products are GC peak areas in area-percent.

Table 4. High Temperature Pyrolysis Products as Eluted on GC.

Retention time (min)	4 (%4)	8 (%8)	9 (%9)	14 (%14)	15 (%15)	16 (%16)	17 (%17)	18 (%18)	19 (%19)	20 (%20)
0	PG, HCN, H2O 88.9	PG, H2O 69.8	PG, HCN, H2O 85.9	PG, H2O 74.7	PG 59.6	PG, H2O 91.6	PG 61.4	PG 43.7	PG, HCN, H2O 84.2	PG, HCN, H2O 59.4
0.5					CH3CHO 22.4			CH3CHO 15.3		
1				HNCO 0.2						
1.5					HNCO 3.8	acrolein 0.8		HNCO 3.7	HNCO 1.6	
2	HNCO 0.4		HNCO 1.4		C=O 4.5		acrolein 0.6	acetone 7.5	acrolein 0.7	
2.5							triazine 2.0			
3				NH3 4.4						
3.5						RNO3 0.2	HCOOH 0.2	acrolein 3.7		triazine 2.1
4		triazine 6.3								CH3COOH 1.1
4.5						benzene 0.3		nitro- 2.2		
5			triazine 3.6			aldehyde 0.3		methane		
5.5						triazine 5.7		CH3COOH 9.3		
6			HCOOH 0.1	triazine 2.2	RNCO 0.6		C=O			HCOOH 11.6
6.5					CH3COOH 4.5		.			
7	triazine 8.9						. 25.4	C=O 1.9		
7.5				HCOOH 1.5		toluene 0.2	.		triazine 9.8	
8		C=O, C=O 17.1					C=O	nitro- 1.5		
8.5								ethane		C=O 17.6
9					RNCO 0.6					C=O 1.5
9.5			C=O							C=O 0.5
10			.					C=O 1.1		C=O 0.4
10.5		nitro- 3.6	.			L=O 0.3	nitro- 6.8			
11		formamine	.				formamine	RNCO 1.1		nitro-
11.5			. 9.8							formamine 0.6
12			.	C=O	RNCO 1.3			C=O 1.9		RNCO 0.2
12.5		RNCO 0.6	.	.						
13			.	.		C=O, C=O 0.3 0.3	C=O	C=O, C=O 1.5 1.5		C=O, C=O 2.1
13.5			.	.			. 2.9		C=O 1.8	
14	C=O		C=O	. 16.5			C=O			C=O
14.5	. 1.6			.				RNCO 3.4		C=O 2.6
15	C=O	C=O, C=O 2.6		.	RNCO 1.3		C=O			
15.5				.			. 3.9			
16				C=O	RNCO 1.3		C=O	C=O 0.7	C=O 2.7	
16.5										
17										
17.5										C=O 0.5
18										
18.5										

21	%(21)	22	(%22)	23	(%23)	24	(%24)	25	(%25)	RDX	(%RDX)	HMX	(%HMX)	GAP	(%GAP)	HTPB	(%HTPB)	time(min)
PG HCN	72.8	PG H2O H2O	71.0	PG	62.8	PG HCN H2O	74.8	PG HCN H2O	72.4	PG HNCO RNO3 triazine	26.4 24.2 3.1 6.3	PG HCN H2O	44.3	PG	38.7	PG monomer	10.6 22.7	0 0.5
														CH3CHO	28.1			1
								HNCO	0.5			HNCO acetone	3.2 1.3	HNCO acetone	7.8 4.8			1.5 2 2.5
		triazine	2.5	triazine	3.3	triazine	1.5			C=O	4.1							3
triazine	4.0	CH3COOH	3.2	CH3COOH	2.5	CH3COOH	1.5			C=O	0.6	triazine	1.3					3.5
CH3COOH	1.0									C=O	0.3					dimer	14.4	4
										C=O	21.9							4.5
HCOOH	5.0	HCOOH	3.8			HCOOH	2.5			C=O . . .	13.1					alkene	2.3	5 5.5 6
				HCOOH	7.1					.		HCOOH	2.9					6.5
C=O . . . C=O	14.6	C=O . C=O	14.8	C=O C=O C=O	14.6 2.0 0.6	C=O C=O RNO3 C=O C=O	14.8 1.5 0.9	CH3COOH triazine	0.2 7.4	. . . C=O						aromatic alkene alkene	3.0 5.3 2.3	7 7.5 8 8.5 9 9.5
				HCOOH C=O	0.4 0.9													10
C=O	0.1	C=O	1.9	C=O		C=O								RCH=NH	3.2			10.5
nitro- formamine	0.6	C=O		nitro- formamine	0.7	. . C=O	1.0					C=O	6.7					11
		C=O	1.1	C=O . . C=O	2.5			C=O . . .	17.4			C=O C=O	12.8	C=O C=O	4.4 6.3			11.5 12 12.5
C=O	1.8																	13 13.5
C=O	0.6	C=O . . . C=O	1.0	C=O . . . . . C=O	2.6	C=O . . . . . C=O	1.0	C=O				C=O . . . . C=O	27.4	C=O	3.8	alkene alkene alkene alkene	11.3 4.5 6.8 3.8	14 14.5 15 15.5 16 16.5
																RNCO	13.6	17 17.5
C=O	0.1													RNCO	3.6			18 18.5

Key:

PG	permanent gases	C=O	carbonyl compounds (amides, ketones, aldehydes)
RNCO	isocyanates	RNO3	nitrates
RCH=NH	imines	CH3COOH	acetic acid
HCOOH	formic acid	CH3CHO	acetaldehyde
HCN	hydrogen cyanide	HNCO	isocyanic acid
monomer	butadiene monomer	dimer	butadiene dimer

] Overlapping peaks; GC peak areas have been summed.

NOTE: Pyroprobe set temperature: 1,000° C for all formulations. Retention times have been rounded off to the nearest 0.5 min. Numbers appearing to the right of products are GC peak areas in area-percent.

Table 5. Pyrolysis Products for Low Temperature Experiments

Sample No.	PG, HCN and H_2O	Triazine	RNO_2	RNO_3	RCOOH	RNCO and HNCO	C=O[b]
	(GC area-percent)						
4	79.8	0.0	0.0	11.3	2.6	1.6	3.4
8	46.7	21.2	0.0	0.0	7.0	4.0	21.2
9	81.0	0.0	7.3	0.4	0.4	1.4	7.6
14[a]	56.2	1.4	7.9	0.0	0.0	0.0	25.8
15	85.0	0.0	0.0	0.0	4.6	1.5	8.6
16	50.6	14.6	5.6	0.0	0.5	0.0	28.8
17	69.2	5.7	5.1	0.0	0.0	0.0	20.0
18	67.1	0.0	1.9	0.0	5.7	5.2	20.2
19	90.6	0.0	0.0	4.5	0.0	2.9	1.3
20	80.7	1.4	0.0	0.0	0.8	0.0	17.2
21	85.0	0.3	0.0	0.0	2.4	0.0	13.3
22	70.0	6.9	0.4	0.0	0.0	0.0	22.0
23	57.2	3.2	0.0	0.0	8.5	0.0	31.1
24	71.3	2.5	0.4	8.2	7.3	0.0	10.6
25	82.8	0.0	0.0	9.7	0.0	5.7	1.8
RDX	29.9	8.1	8.0	0.0	4.6	0.0	49.5
HMX	92.1	2.3	0.0	0.0	0.0	0.0	5.7

[a]Also gave 7% ether.

[b]Amides, ketones, and aldehydes.

Table 6. Pyrolysis Products for High Temperature Experiments

Sample No.	PG, HCN and H_2O	Triazine	RNO_2	RNO_3	RCOOH	RNCO and HNCO	C=O[b]
	(GC area-percent)						
4	88.9	8.9	0.0	0.0	0.0	0.6	1.6
8	69.8	6.3	3.6	0.0	0.0	0.6	19.8
9	85.9	3.6	0.0	0.0	0.1	1.4	9.0
14	79.1	2.2	0.0	0.0	1.5	0.2	16.5
15	59.6	0.0	0.0	0.0	4.5	8.9	26.9
16	91.6	5.7	0.2	0.0	0.0	0.0	2.0
17	61.4	2.0	4.8	0.0	0.2	0.0	32.8
18	43.7	0.0	4.1	0.0	9.3	8.2	35.1
19	84.2	9.0	0.0	0.0	0.0	1.6	5.2
20	59.4	2.1	0.6	0.0	12.7	0.2	24.3
21	72.8	4.0	0.6	0.0	6.0	0.0	16.4
22	71.0	2.5	0.0	0.0	7.0	0.0	18.8
23	62.8	3.3	1.7	0.0	9.6	0.0	23.2
24	74.8	1.5	0.0	1.5	4.0	0.0	17.7
25	72.7	7.4	0.0	0.0	0.2	0.5	17.2
RDX	26.4	6.3	3.1	0.0	0.0	24.2	40.0
HMX	44.4	1.3	0.0	0.0	2.9	3.2	48.2
GAP	38.7	0.0	0.0	0.0	0.0	7.0	51.0
HTPB[a]	10.6	0.0	0.0	0.0	0.0	13.6	0.0

[a]Also gave 22.7% butadiene monomer, 14.4% butadiene dimer, 2.3% unidentified alkane, 33.2% unidentified alkene, 3.0% unidentified aromatic.

[b]Amides, ketones, and aldehydes.

Table 7. Individual Permanent Gas Pyrolysis Products for Low Temperature Experiments

Sample No.	CH_4	CH_2O	CO_2	N_2O	CO	NO
	Normalized IR Absorbance					
4	0.00	0.14	0.45	0.25	0.01	0.03
9	0.03	0.00	0.43	0.38	0.06	0.09
14	0.06	0.00	0.37	0.43	0.06	0.08
17	0.03	0.00	0.38	0.45	0.04	0.09
19	0.00	0.07	0.45	0.34	0.03	0.05
20	0.05	0.00	0.39	0.41	0.07	0.09
21	0.04	0.00	0.40	0.40	0.07	0.09
22	0.07	0.00	0.38	0.41	0.06	0.09
24	0.06	0.00	0.39	0.42	0.06	0.08
25	0.00	0.16	0.32	0.32	0.02	0.05

NOTE: Permanent gas data tabulated only for those samples for which ignition data were available.

Table 8. Individual Permanent Gas Pyrolysis Products for High Temperature Experiments

Sample No.	CH_4	CH_2O	CO_2	N_2O	CO	NO
	Normalized IR Absorbance					
4	0.05	0.00	0.39	0.40	0.07	0.12
9	0.03	0.00	0.43	0.40	0.06	0.08
14	0.08	0.00	0.38	0.47	0.07	0.09
17	0.13	0.00	0.40	0.34	0.05	0.09
19	0.07	0.00	0.40	0.37	0.07	0.10
20	0.06	0.00	0.45	0.33	0.07	0.09
21	0.06	0.00	0.41	0.35	0.07	0.10
22	0.08	0.00	0.39	0.37	0.07	0.10
24	0.08	0.00	0.40	0.33	0.08	0.11
25	0.06	0.00	0.41	0.37	0.07	0.09

NOTE: Permanent gas data tabulated only for those samples for which ignition data were available.

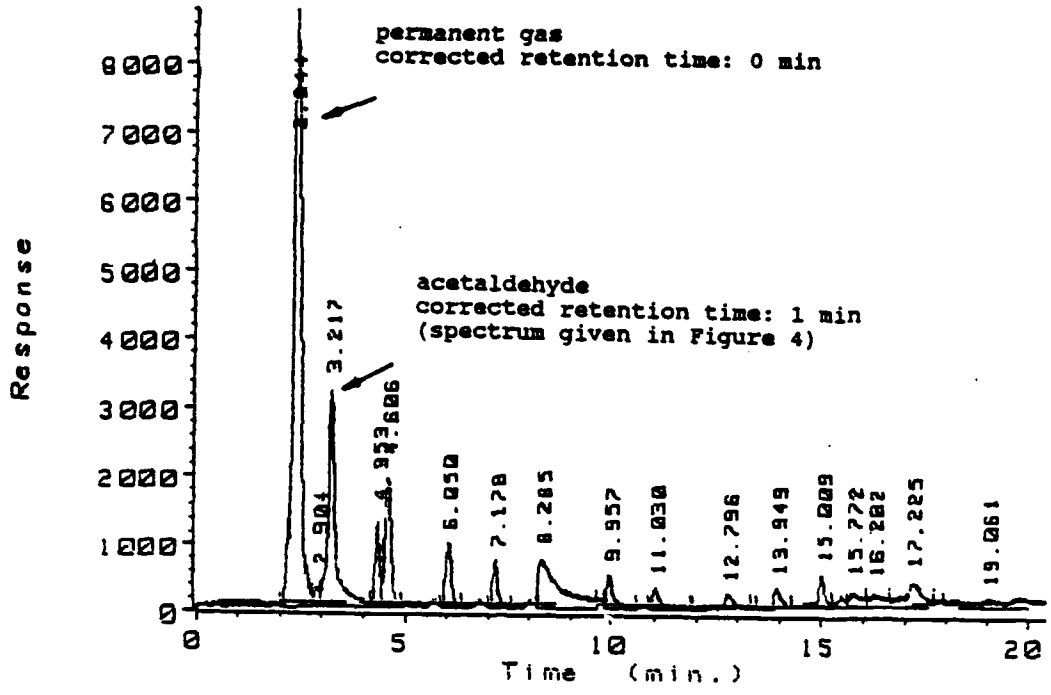

Figure 3. Example of a GC-FTIR Chromatogram. Sample 18 Pyrolyzed at 1,000° C. Permanent Gas and Acetaldehyde Peaks Labelled.

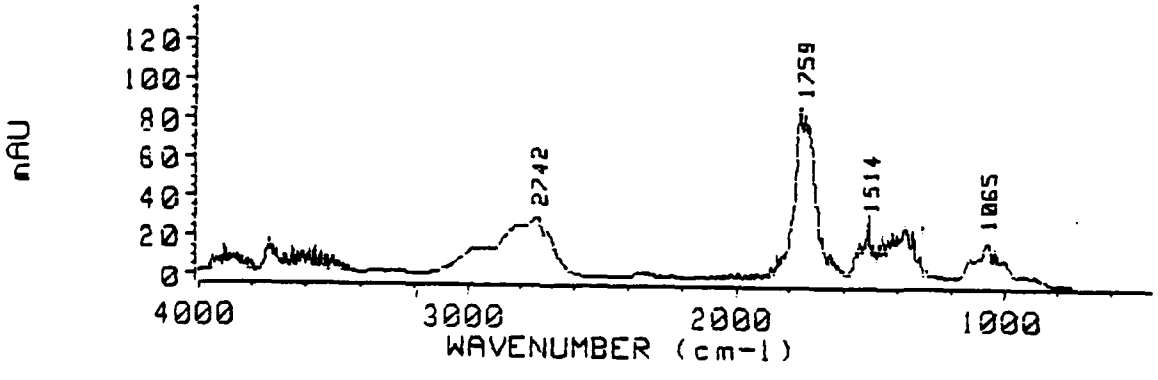

Figure 4. Example of an FTIR Spectrum Used to Identify Pyrolysis Products. Sample 18 Pyrolyzed at 1,000° C; Corrected Retention Time = 1 min; Peak Assignment: Acetaldehyde.

Observed trends in pyrolysis product distributions are listed as follows:

In low temperature pyrolysis experiments:

(1) RDX-based formulations generally gave larger yields of CO_2 and smaller yields of N_2O, CO, NO, and CH_4 than HMX-based formulations.

(2) Formaldehyde was observed only for plasticized RDX formulations. Those same RDX formulations yielded no CH_4.

(3) Formulations composed of only GAP and plasticizer (samples 15 and 18) did not generate formaldehyde.

(4) HMX and all HMX formulations yielded HCN, but neither RDX nor any of the RDX formulations did.

(5) All samples except 8, 15, and 18 gave water as a pyrolysis product.

(6) Unplasticized formulations had the lowest permanent gas yields (samples 8, 14, 16, and 17).

(7) Samples plasticized with BTTN (9, 19, 20, and 21) had larger permanent gas yields than those plasticized with TMETN.

(8) Samples with large yields of permanent gases were found to have low yields of carbonyl compounds.

(9) Nitrates appeared as pyrolysis products for only sample 24 (HMX/GAP/TMETN) and the four plasticized RDX/GAP formulations (samples 4, 9, 19, and 25).

(10) Plasticized RDX/GAP formulations were the only samples that gave no triazine (except for samples 15 and 18 which contained no oxidizer and were not expected to give triazine).

(11) Isocyanate products did not appear for any HMX based formulations. All but one RDX-based formulation (sample 16, RDX/HTPB) gave isocyanate pyrolysis products.

(12) Samples of pure RDX and HMX pyrolyzed at 400° C and 500° C, respectively, gave strikingly different amounts of permanent gases, i.e., RDX ~30 area-percent and HMX ~90 area-percent.

In high temperature pyrolysis experiments:

(1) Formulation appeared to have little effect on yields of individual permanent gases.

(2) Plasticized RDX formulations (4, 9, 19, and 25) produced HCN, but unplasticized RDX formulations (8 and 16) did not.

(3) HCN was produced for all HMX formulations except 17, 21, and 23.

(4) Yields of carboxylic acids and isocyanates were generally larger than in low temperature experiments.

(5) As in the low temperature experiments, there was an inverse relationship between the yields of permanent gases and carbonyl compounds.

(6) Nitrates were observed only for sample 24 (HMX/GAP/TMETN).

(7) RDX and HMX both generated a relatively low yield of permanent gas.

(8) RDX and HMX differed greatly in the amount of HNCO produced, i.e., 24.2 and 3.2 area-percent, respectively.

(9) GAP yielded small amounts of total permanent gas, but large amounts of carbonyl compounds, the majority of which were acetaldehyde and acetone.

(10) Most carbonyl products for RDX had retention times of 5 to 9 min. For HMX, most had times of 11 to 18 min.

(11) The distribution for HTPB consisted primarily of alkenes, including butadiene monomer, dimer, and several monounsaturated compounds.

(12) For unplasticized samples (8, 14, and 16) levels of permanent gases, including HCN and H_2O, were higher than in low temperature experiments.

(13) The permanent gas level for samples 15 and 18 (50% GAP/50% plasticizer) were much lower than for low temperature experiments.

(14) For plasticized samples (with an oxidizer), the permanent gas level in high and low temperature experiments generally differed by less than 10 area-percent.

(15) All samples containing either RDX or HMX generated triazine as a pyrolysis product.

3.2 Selection of Performance Data for Correlation With Pyrolysis Products. The performance test results provided by NWC are given in Table 9. They consist of impact sensitivity and burn rate measurements as well as "first light" and "go/no-go" ignition times. First light measurements indicate initial emission whereas go/no-go measurements indicate the time of laser stimulus necessary for 50% of the samples to sustain combustion after removal of the stimulus. Theoretical specific impulse was also provided. Plots of burn rate and impact sensitivity vs. specific impulse (Figures 5 and 6, respectively) indicate a strong correlation and suggest that these two measurements are thermodynamically controlled. First light and go/no-go ignition times (Figures 7 and 8, respectively) do not show such a correlation and are therefore not believed to be thermodynamically controlled, making them suitable choices for possible correlations with pyrolysis product distributions.

Table 9. NWC Performance Test Results

Sample No.	I_{sp}[a] (1/s)	Impact (cm)	Burn Rate[b] (mm/s)	Ignition Times							
				Go/No-Go (ms)				First Light (ms)			
				60[c]	100[c]	150[c]	200[c]	60[c]	100[c]	150[c]	200[c]
4	257.8	13.6	7.9	11.5	5.8	4.7	8.0	10.3	5.1	2.4	1.5
8	236.4	30.2	6.6	Na	Na	Na	Na	Na	Na	Na	Na
9	257.0	15.6	7.6	9.9	5.1	3.4	6.1	8.9	4.2	1.5	0.6
14	235.8	23.4	7.1	43.64	50.36	70.36	86.43	9.11	3.92	2.67	1.28
15	221.4	33.9	Na	Na	Na	Na	Na	Na	Na	Na	Na
16	213.9	41.6	Na	Na	Na	Na	Na	Na	Na	Na	Na
17	214.6	25.7	3.6	22.43	22.64	17.14	11.07	7.81	4.92	2.37	1.46
18	216.7	51.3	Na	Na	Na	Na	Na	Na	Na	Na	Na
19	251.0	22.9	7.1	8.21	4.5	4.21	5.37	6.27	3.67	2.28	0.98
20	251.3	21.9	7.9	10.21	7.33	10.83	17.70	6.72	3.84	2.12	1.18
21	246.3	18.6	7.4	11.5	8.17	8.50	13.00	7.12	4.65	2.84	1.47
22	243.1	17.0	6.9	15.83	20.50	33.21	53.21	7.03	5.09	3.15	1.31
23	241.6	20.9	Na	Na	Na	Na	Na	Na	Na	Na	Na
24	249.1	20.6	6.6	14.36	20.83	18.50	20.7	9.43	4.10	2.74	1.91
25	248.8	21.3	6.4	10.64	13.07	21.64	29.5	8.00	3.92	2.01	1.89

Na = not available

Source: Yee (1988)

[a] I_{sp} - Theoretical specific impulse.

[b] Measured at 1,000 psi.

[c] All ignition times at specified laser flux (cal/m^{2}s), measured at 250 psi.

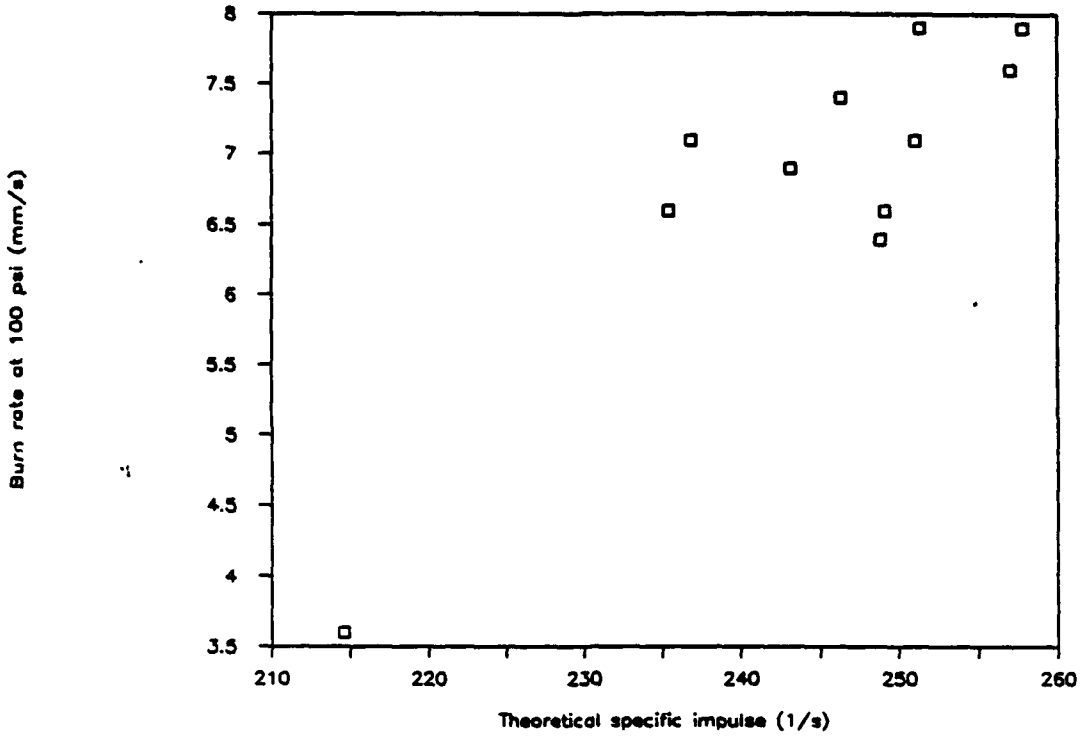

Figure 5. NWC Burn Rate Data vs. Theoretical Specific Impulse.

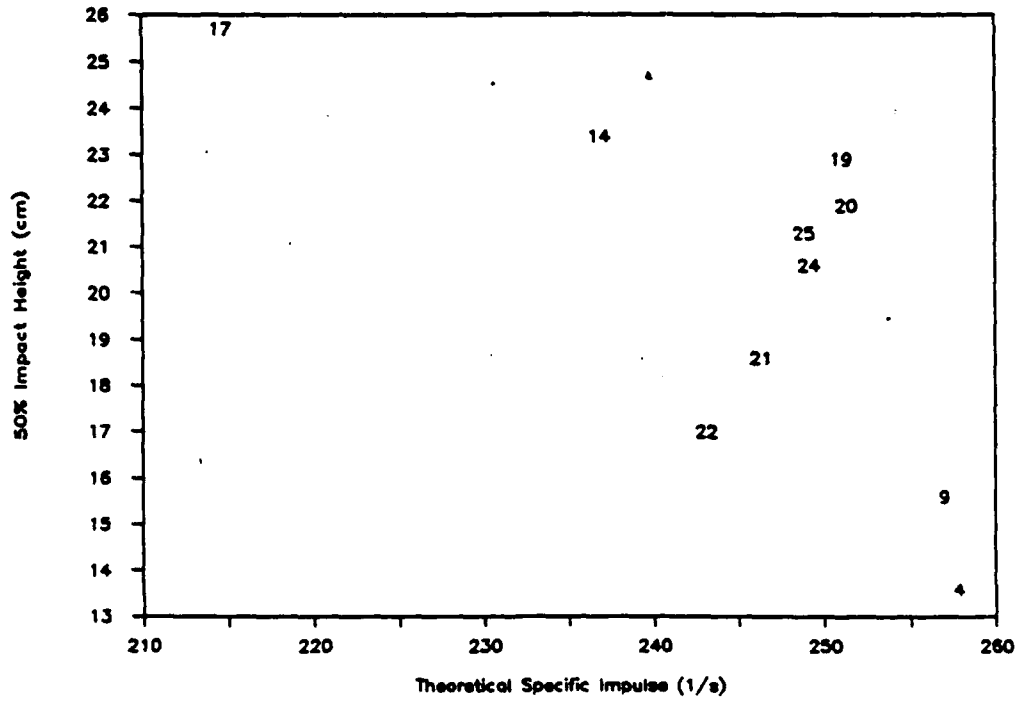

Figure 6. NWC Impact Sensitivity Data vs. Theoretical Specific Impulse.

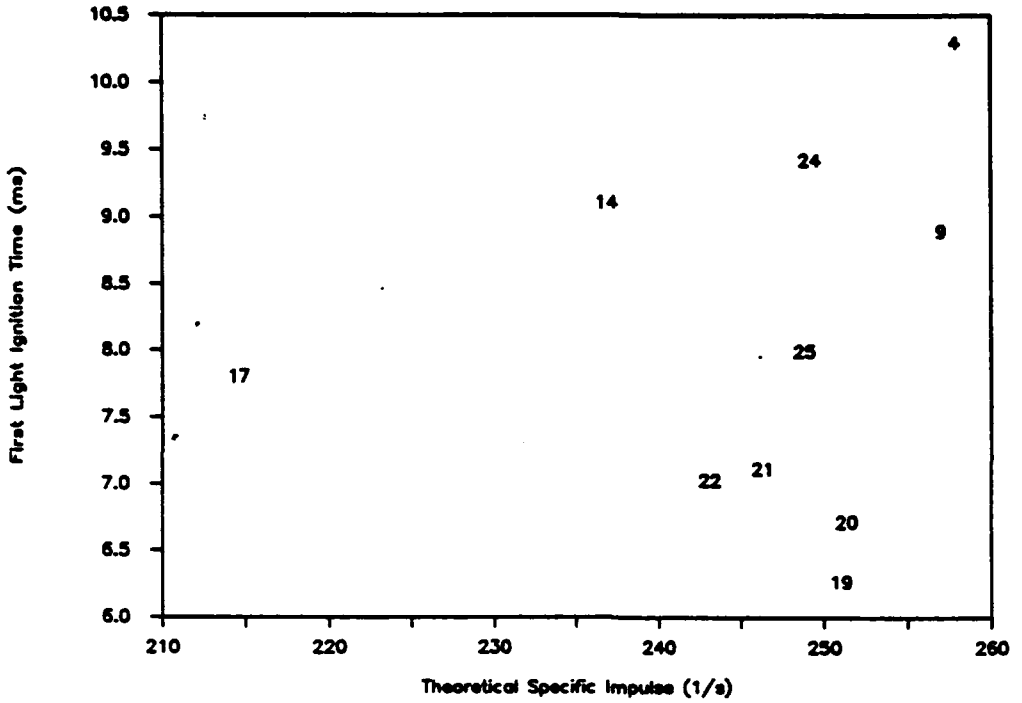

Figure 7. NWC First Light Ignition Data (60 cal/m^{2}s) vs. Theoretical Specific Impulse.

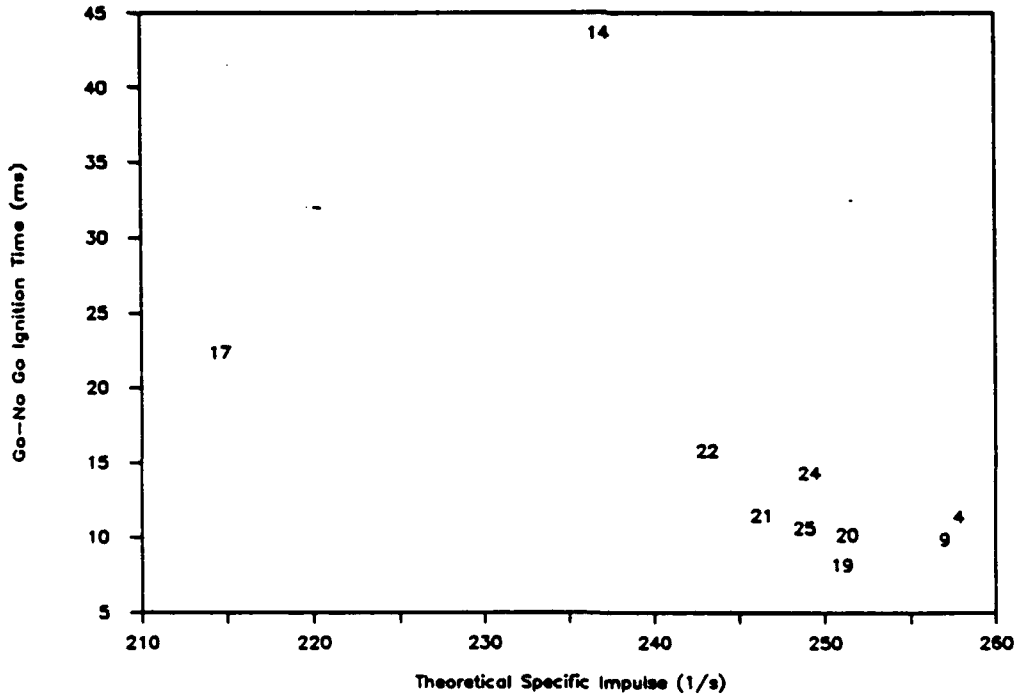

Figure 8. NWC Go-No Go Ignition Time (60 cal/m^{2}s) vs. Theoretical Specific Impulse.

3.3 Correlation of Pyrolysis Products and Ignition Data. To identify correlations, several techniques and tools were used. These include simple visual examination of P-GC-FTIR data in formats similar to those used for Tables 3 and 4, as well as a multitude of plots generated by a spreadsheet program (Symphony) and two multivariate analysis packages (Ein*Sight and Minitab). Possible correlations for all pyrolysis products vs. all ignition data were explored. Plots of percent pyrolysis product for total permanent gases and carbonyl compounds vs. ignition time (flux: 60 cal/m^{2}s) are given in Figures 9 and 10, respectively. The best correlation is observed for total permanent gases (low temperature products) vs. low flux (60 cal/m^{2}s) go/no-go ignition times. Fairly good correlations with go/no-go times are also observed for the carbonyl compounds. The most general explanation for these results is that cleaner burning samples produce more small decomposition products (like permanent gases) than large fragments (such as carbonyl compounds), resulting in shorter go/no-go ignition times due to higher surface temperatures.

Correlation of total permanent gases production with go/no-go ignition times at laser fluxes >60 cal/m^{2}s were also observed, but were not as good as that for the lowest laser flux presumably due to ablation and/or overdriven ignition (Cosgrove and Owen 1974), at the higher fluxes. No significant correlations were observed for any of the high temperature pyrolysis products when plotted against either go/no-go or first light ignition times, nor were any observed for low temperature products when plotted against first light ignition times. Differences between high and low temperature pyrolysis product distributions are discussed above, but do not explain the lack of correlation with first light ignition times.

4. DISCUSSION

There are several striking differences in the low temperature pyrolysis product distributions for RDX and HMX formulations. Most are likely due to differences in reaction temperature. All RDX-based formulations were pyrolyzed at a set temperature that was 100° C lower than for HMX formulations. This was done to compensate for the difference in oxidizer melting points (204° C and 280° C for RDX and HMX, respectively). Since HMX and RDX rapidly decompose at their melting points, HMX is at a temperature almost 100° C higher than RDX when it actually melts. This could explain the large difference in permament gas yields between RDX and HMX, i.e., 29.9 and 92.1 area-percent, respectively. Based on the notion

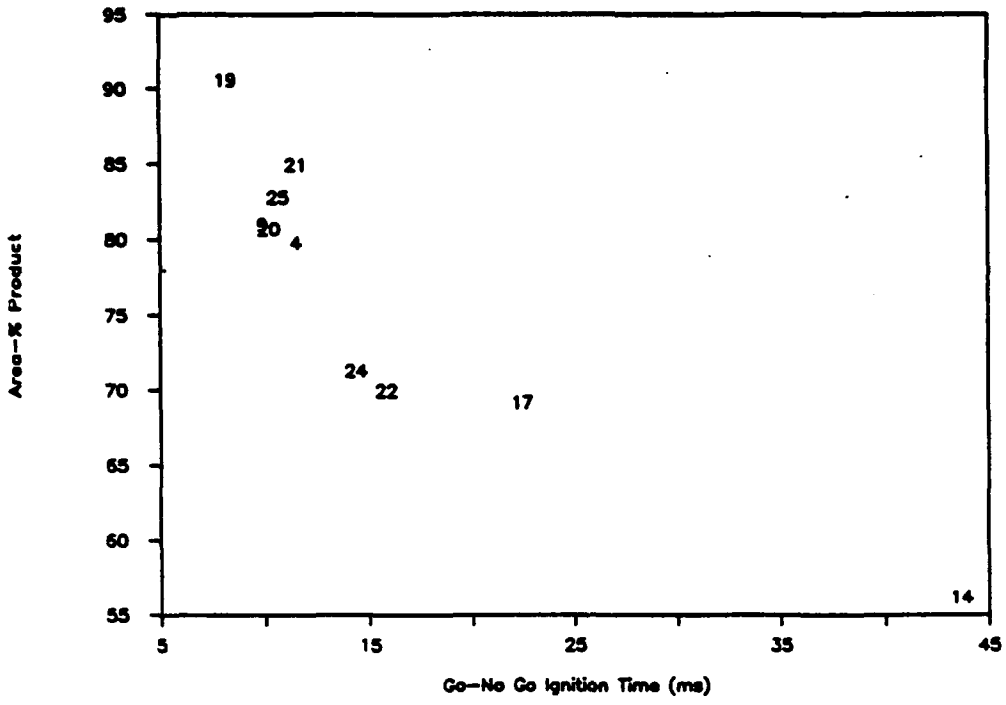

Figure 9. Correlation Plot. Low Temperature Permanent Gas Products vs. Go/No-Go Ignition Time (60 cm/m^{2}s flux).

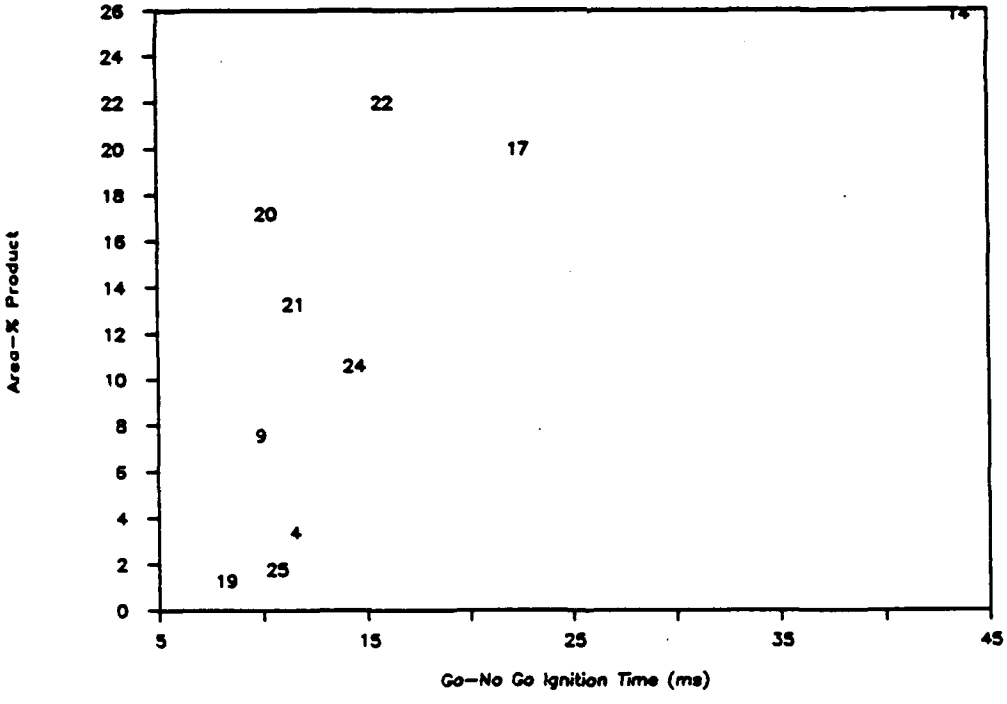

Figure 10. Correlation Plot. Low Temperature Carbonyl Compounds vs. Go/No-Go Ignition Time (60 cm/m^{2}s).

that N-N bond rupture dominates at higher temperatures and that C-N rupture dominates at lower temperatures, this may also explain why in low temperature pyrolysis experiments RDX formulations generate formaldehyde while HMX formulations do not, and similarly why HMX formulations generate HCN while RDX formulations do not.

Examination of go/no-go ignition times as a function of laser flux suggests that samples can be divided into three groups (see Figures 11–13). Group I (samples 14, 22, 25, and 24) exhibits increasing go/no-go times with increasing flux. Group II (samples 20, 21, 4, 9, and 19) has ignition times that first decrease and then increase with increasing flux. (Ignition times at a flux of 200 cal/m^{2}s for HMX formulations increase to values larger than those at 60 cal/m^{2}s while ignition times at 200 cal/m^{2}s for the RDX formulations in this group increase to values smaller than those at 60 cal/m^{2}s). Group III is composed only of sample 17 (the unplasticized sample formulated with HTPB) and exhibits go/no-go ignition times that decrease with increasing laser flux. Observations described below suggest that differences in ignition behavior exhibited by these groups are related to ablation and/or overdriven ignition at high laser fluxes, as well as to the ability of plasticizer and/or plasticizer decomposition products to catalyze propellant decomposition. Pyrolysis GC-FTIR investigation of BTTN and TMETN decomposition at 400° C reveals the production of permanent gases, including a relatively large amount of formaldehyde, as well as several nitrate ester fragments. Which, if any, of these products may serve as catalysts has not been determined, though formaldehyde has been reported to catalyze the thermal decomposition of RDX (Batten 1971a, 1971b; Liebman et al. 1987). Further evidence of catalysis by plasticizer and/or plasticizer decomposition products is the observation that while triazine is produced for HMX formulations and unplasticized RDX formulations in low temperature experiments, as well as for all HMX and RDX formulations in high temperature experiments, no triazine is produced for plasticized RDX formulations at low temperature. Based on a comparison of the amount of nitrate fragments produced as a result of low and high temperature pyrolysis ("RNO_3" in Tables 5 and 6), it appears that plasticizer decomposition is more complete for high temperature pyrolysis. Other than sample 24 (HMX/GAP/TMETN), the only samples giving nitrate decomposition products are the plasticized RDX formulations (4, 9, 19, and 25), and they do so only when pyrolyzed at low temperature. These same formulations happen to be the same samples that do not give triazine. These observations seem to suggest catalytic properties of nitrates (see Scheme 1). In a related study that examined the thermal decomposition of RDX

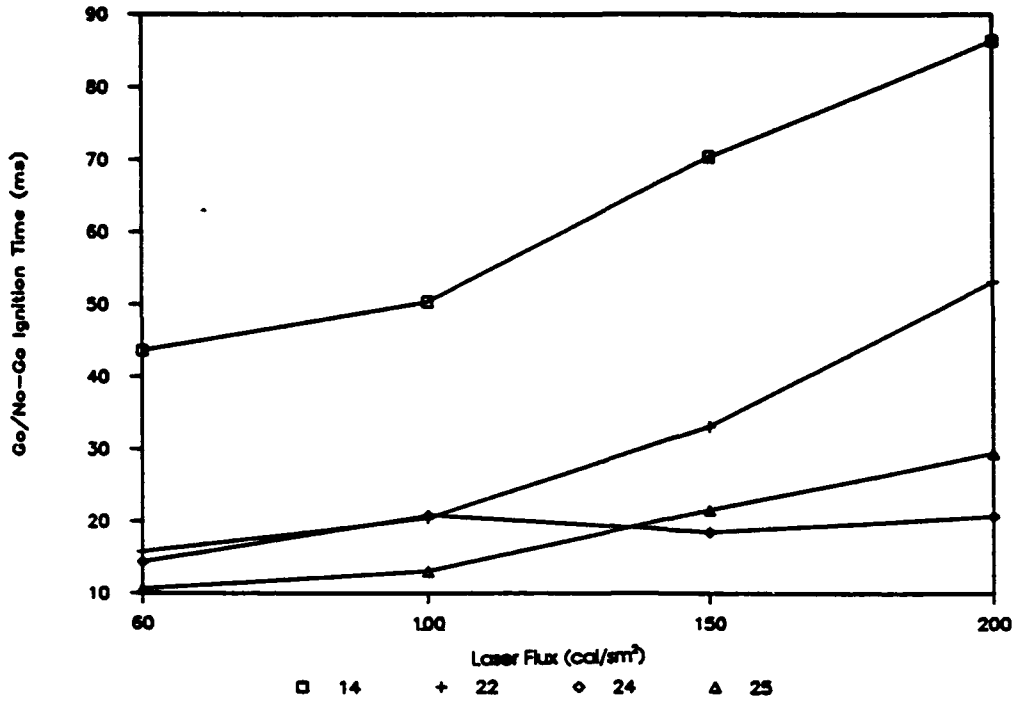

Figure 11. NWC Go/No-Go Ignition Time vs. Laser Flux for Group I.

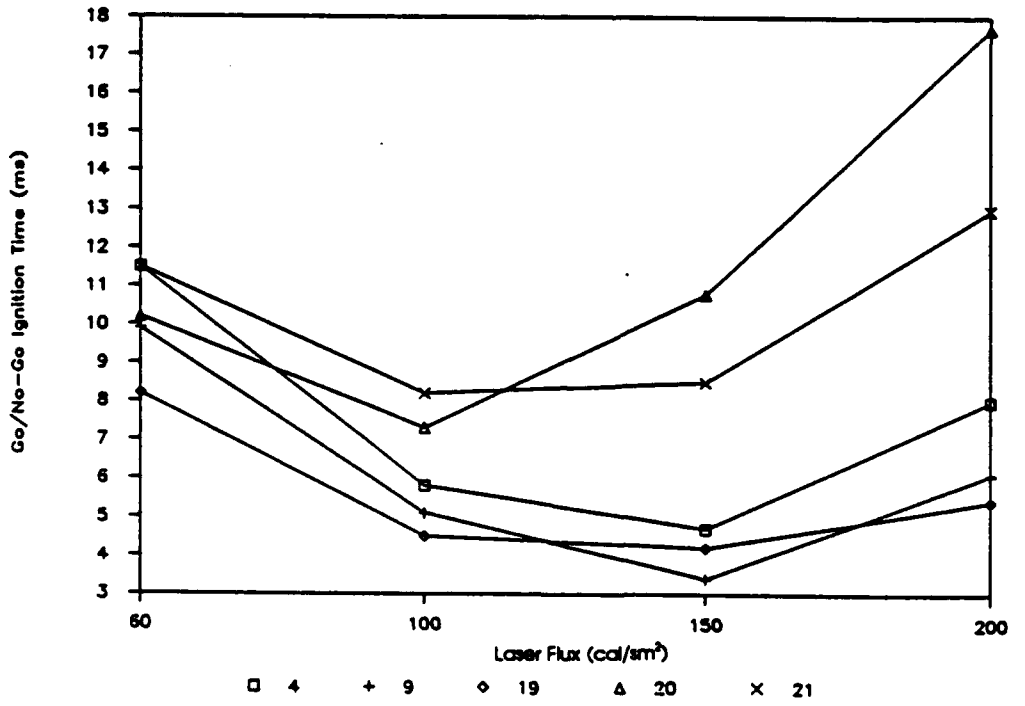

Figure 12. NWC Go/No-Go Ignition Time vs. Laser Flux for Group II.

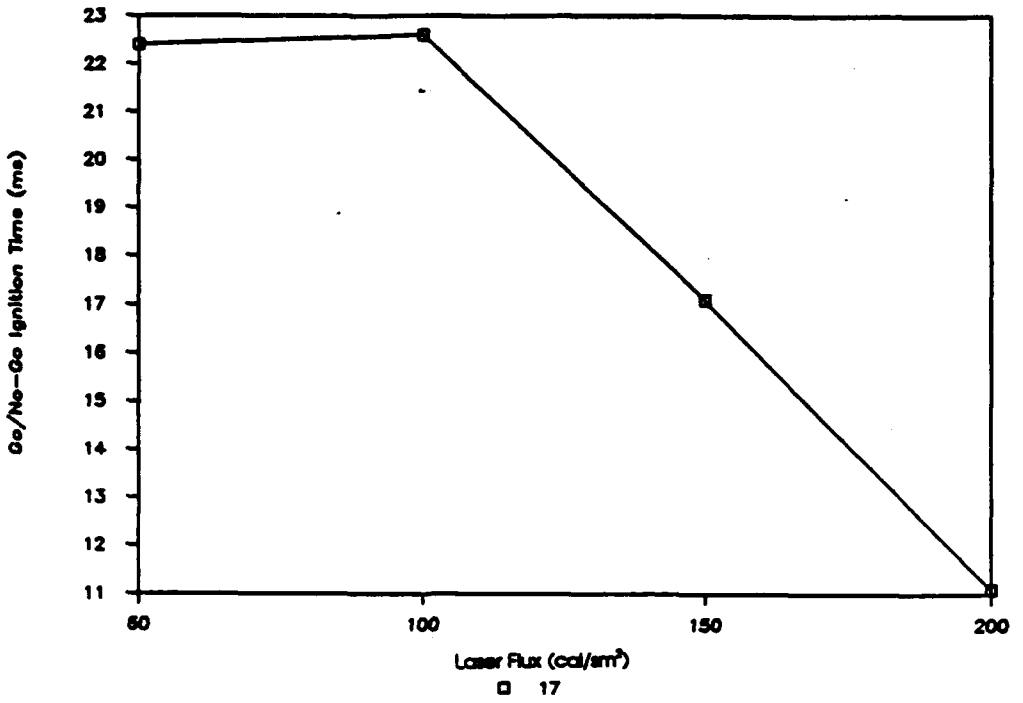

Figure 13. NWC Go/No-Go Ignition Time vs. Laser Flux for Group III.

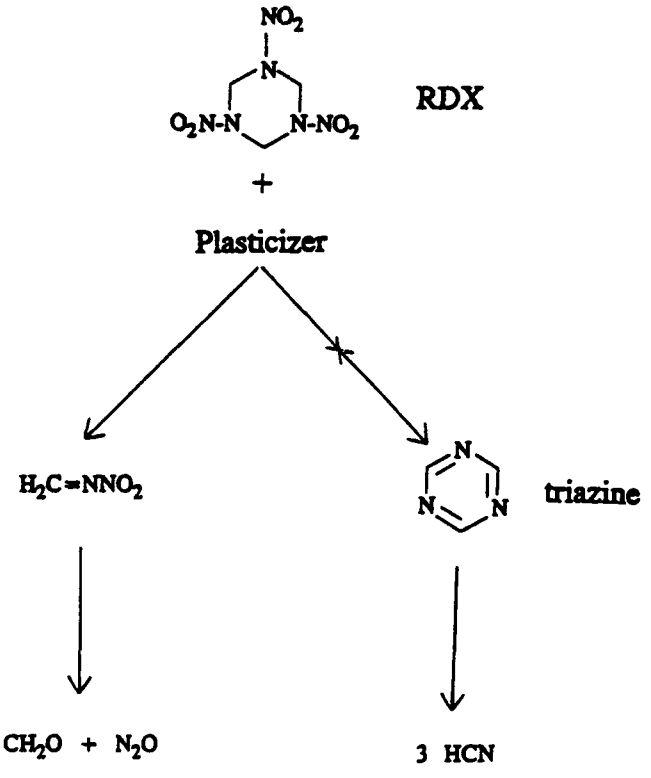

Scheme 1.

with GC-MS (Liebman et al. 1987), it was found that the presence of borohydride catalysts eliminated both triazine oxide and NO_2 from the decomposition products.

It is observed that Group I contains an unplasticized formulation (sample 14) and TMETN plasticized formulations, but no BTTN plasticized formulations. Group II is composed almost exclusively of BTTN plasticized formulations (the one TMETN plasticized sample in Group II, sample 4, differs from other TMETN samples in that it is formulated with only about one-third the amount of GAP).

Although both BTTN and TMETN are both energetic plasticizers, BTTN is the more sensitive of the two as evidenced by the impact sensitivities for samples 15 (GAP/BTTN) and 18 (GAP/TMETN), i.e., 33.9 and 51.3 cm, respectively (Table 9). It is conceivable that since BTTN is the more sensitive plasticizer, it will decompose more readily at lower laser fluxes than will TMETN. Its decomposition products will then be available to catalyze decomposition of the rest of the sample. At high laser fluxes, increased temperatures encourage more rapid, but perhaps less efficient, decomposition of the entire formulation. At sufficient flux, material will ablate from the sample and remove heat from the reaction zone, resulting in the increased ignition times observed for Group I at all fluxes and Group II at high fluxes.

Similar reasoning may explain the production of acetaldehyde (CH_3CHO) by samples 15, 18 and GAP in high temperature experiments (Table 8), retention time: 1.5 min), but by only sample 18 in low temperature experiments (Table 7), note that GAP was not pyrolyzed at low temperature. In the low temperature experiment, sample 15 (GAP/BTTN) produces large amounts of permanent gases, but no acetaldehyde, indicating more complete decomposition of GAP than for sample 18 (GAP/TMETN) which produces a significant amount of acetaldehyde and almost 20% less permanent gases. In high temperature experiments, where decomposition is probably instantaneous, plasticizer does not have the opportunity to catalyze GAP decomposition. The result is that samples 15 and 18 decompose less efficiently and generate almost as much acetaldehyde as unplasticized GAP (22.4, 15.5, and 28.1%, respectively for samples 15, 18, and GAP). Samples 15 and 18 also generate relatively small amounts of permanent gases, though more than does unplasticized GAP (59.6, 43.7, and 38.7%, respectively for samples 15, 18, and GAP).

The observation that samples plasticized with BTTN tend to have shorter first light times than unplasticized formulations or those plasticized with TMETN (Table 9) may lend further support to the ideas proposed here.

Sample 17 does not fit into either Group I or II. It is the only sample that demonstrates decreasing ignition times with increasing flux. This suggests that ablation is not a problem for this unplasticized, HTPB-bound formulation. Two additional unplasticized, HTPB-bound samples (Yee, private communication) prepared along with those in this study, but not examined by us, show a similar trend and indicate that the behavior is not unique to sample 17, but rather is a characteristic of HTPB-bound formulations.

5. CONCLUSION

The primary objective of this investigation was to identify correlations between ignition times and pyrolysis product distributions. Such correlations have been found for go/no-go ignition times, but not for first light ignition times. The reason for lack of correlation with first light measurements is not clear. An explanation is not necessary for a non-mechanistic study such as this, but would contribute to a more complete understanding of the systems being examined. The correlations that have been identified, namely those of total permanent gases and carbonyl compounds, provide a means for predicting go/no-go ignition times and may be used for small scale screenings of new formulations.

Several trends in pyrolysis product distribution as a function of propellant composition have been observed. Most of these trends are believed to be related to the ability of BTTN and TMETN to catalyze decomposition. Although not directly applicable to performance prediction, the trends and observations reported here are expected to be of interest for those interested in formulation design or propellant decomposition.

6. REFERENCES

Batten, J. J. Australian Journal of Chemistry. Vol. 24, p. 945, 1971a.

Batten, J. J. Australian Journal of Chemistry. Vol. 24, p. 2025, 1971b.

Behrens, R., Jr. "Simultaneous Thermogravimetric Modulated Beam Mass Spectrometry and Time-of-Flight Velocity Spectra Measurements: Thermal Decomposition Mechanisms of RDX and HMX." Proceedings of the 24th JANNAF Combustion Meeting, CPIA Publication 476, vol. I, pp. 333–342, October 1987.

Cosgrove D. J., and A. J. Owen. Combustion and Flame. Vol. 22, pp. 19–22, 1974.

Duff, P. J. "Studies of the Effect of Hivelite and Other Boron Compounds on Nitramine Decomposition by Pyrolysis GC-FTIR." Proceedings of the 22nd JANNAF Combustion Meeting, CPIA Publication 432, vol. II, pp. 547–556, October 1985.

Fifer, R. A. "Chemistry of Nitrate Ester and Nitramine Propellants." Fundamentals of Solid Propellant Combustion, edited by K. K. Kuo and M. Summerfield, vol. 90 of Progress in Astronautics and Aeronautics Series, AIAA, NY, 1984.

Fifer, R. A., S. A. Liebman, P. J. Duff, K. D. Fickie, and M. A. Schroeder. "Thermal Decomposition Mechanisms of Nitramine Propellants." Proceedings of the 22nd JANNAF Combustion Meeting, CPIA Publication 432, vol. II, pp. 537–546, October 1985; see also Journal of Hazardous Materials, vol. 13, pp. 51–56, 1986.

Griffiths, P. R., and J. A. de Haseth. Fourier Transform Infrared Spectroscopy New York: John Wiley and Sons, pp. 604–607, 1986.

Liebman, S. A., A. P. Snyder, J. H. Kremer, D. J. Reutter, M. A. Schroeder, and R. A. Fifer. Journal of Analytical and Applied Pyrolysis, vol. 12, pp. 83–95, 1987.

Morris, J. B., and R. A. Fifer. "An Expert System/CAD Package for Propellant Formulation and Property Estimation." Proceedings of the 27th JANNAF Combustion Meeting, November 1990, in press.

Ohlemiller, T. J., L. H. Caveny, L. DeLuca, and M. Summerfield. "Dynamic Effects on Ignitability Limits of Solid Propellants Subjected to Radiative Heating." Proceedings of the 14th Symposium (International) on Combustion, The Combustion Institute, 20–25 August 1972.

Salo, J. K. "A Thermal Study on the Effect of Thermoplastic Elastomers on LOVA Propellants." Proceedings of the 17th North American Thermal Analysis (NATAS) Conference, vol. II, pp. 779–784, October 1988.

Schroeder, M. A. "Critical Analysis of Nitramine Decomposition Data: Product Distributions from HMX and RDX Decomposition." BRL-TR-2659, U.S Army Ballistic Research Laboratory, Aberdeen Proving Ground, MD, June 1985.

Schroeder, M. A. "Thermal Decomposition of RDX and RDX-$K_2B_{12}H_{12}$ Mixtures." Proceedings of the 23rd JANNAF Combustion Meeting, CPIA Publication 457, vol. II, pp. 43–54, October 1986.

Schroeder, M. A. "Thermal Decomposition of Catalyzed and Uncatalyzed HMX Propellant Formulations." Proceedings of the 24th JANNAF Combustion Meeting, CPIA Publication 476, vol. I, pp. 103-114, October 1987.

Schroeder, M. A. "Borohydride Catalysis of Nitramine Thermal Decomposition and Combustion. III. Literature Review and Wrapup Discussion of Possible Chemical Mechanisms." Proceedings of the 25th JANNAF Combustion Meeting, CPIA Publication 498, vol. III, pp. 421–431, 1988.

Shaw, F. J., and R. A. Fifer. "Pyrolysis GC-FTIR Studies of a LOVA Propellant Formulation Series." BRL-TR-2993, U.S. Army Ballistic Research Laboratory, Aberdeen Proving Ground, MD, May 1989. Proceedings of the 25th JANNAF Combustion Meeting, CPIA Publication 498, vol. III, pp. 409–420, 1988.

Snyder, A. P., J. H. Kremer, S. A. Liebman, M. A. Schroeder, and R. A. Fifer, "Characterization of Cyclotrimethylene-Nitramine (RDX) by N,H Isotope Analysis With Pyrolysis Atmospheric Pressure Ionization Tandem Mass Spectrometry." Organic Mass Spectrometry, vol. 24, pp. 15–21, 1989.

Snyder, A. P., J. H. Kremer, S. A. Liebman, M. A. Schroeder, and R. A. Fifer. "Characterization of Cyclotrimethylenenitramine (RDX) by Pyrolysis H_2O/D_2O Atmospheric Pressure Chemical Ionization Tandem Mass Spectrometry." Organic Mass Spectrometry, vol. 25, pp. 61–66, 1990.

Wise, S., and J. J. Rocchio. "Binder Requirements for Low Vulnerability Propellants." Proceedings of the 18th JANNAF Combustion Meeting, CPIA Publication 347, vol. II, pp. 305–320, October 1981.

Yee, R. Y. "Effects of Surface Interactions and Mechanical Properties of Plastic Bonded Explosives on Explosive Sensitivity. Part 2: Model Formulations." NWC-TP-6619, Naval Weapons Center, March 1985 (ADA 157900).

Yee, R. Y. Private communication, 1988.

Yee, R. Y. "Drop Weight Impact Sensitivity of HMX and RDX as Influenced by Binders and Plasticizers." Proceedings of the 1987 JANNAF Propulsion Systems Hazards Subcommittee Meeting, CPIA Publication 464, vol. I, pp. 253–255, March 1987.

Zhao, X., E. J. Hintsa, and Y. T. Lee. "Infrared Multiphoton Dissociation of RDX in a Molecular Beam." Journal of Chemical Physics, vol. 88, pp. 801–810, 1988.

APPENDIX:

GC-FTIR DATA FOR UNIDENTIFIED PYROLYSIS PRODUCTS

INTENTIONALLY LEFT BLANK.

As discussed in the body of this report, many pyrolysis products could not be identified and are described only by their functionality (i.e., nitro and carbonyl compounds, nitrates, isocyanates). To provide more complete information for future reference, spectra of unidentified products are presented in this appendix. Tables summarizing spectra and associated samples are also given.

Spectrum 1

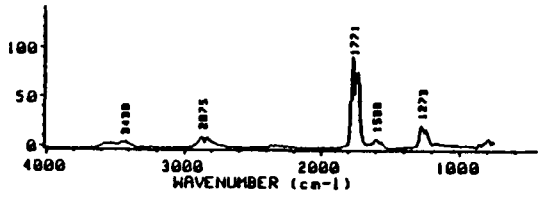

Spectrum 2

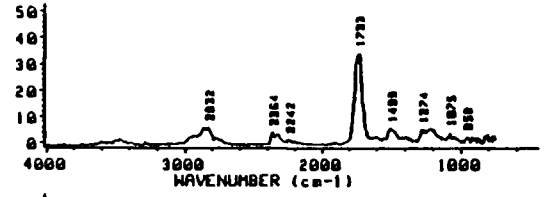

Spectrum 3

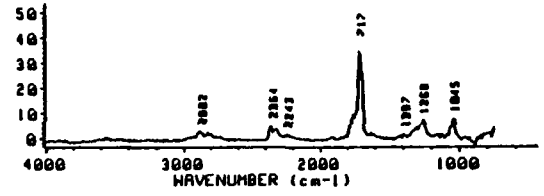

Spectrum 4

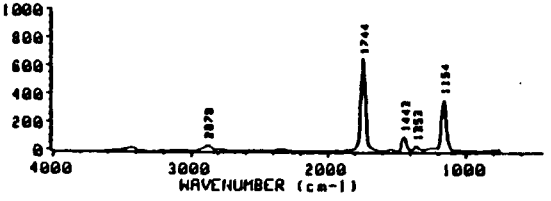

Spectrum 5

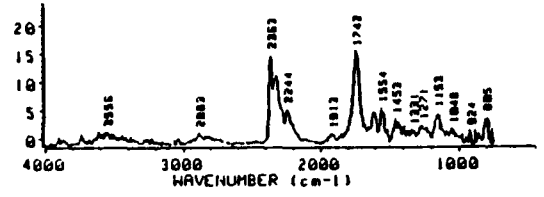

Spectrum 6

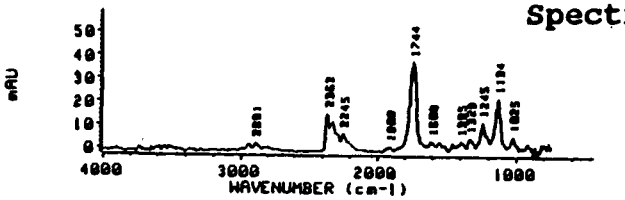

Spectrum 7

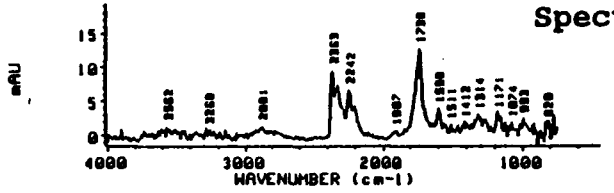

Spectrum 8

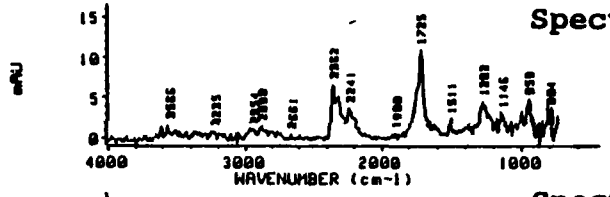

Spectrum 9

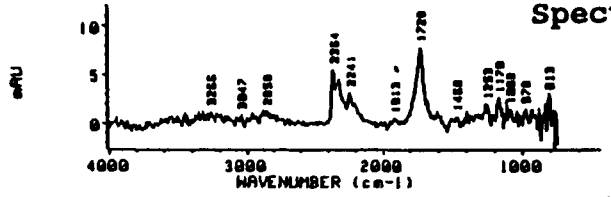

Spectrum 10

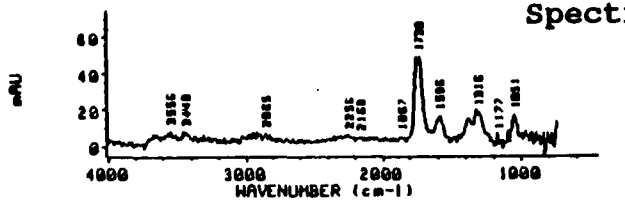

Spectrum 11

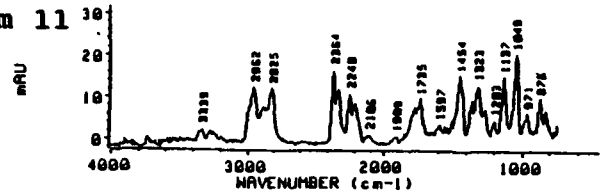

Spectrum 12

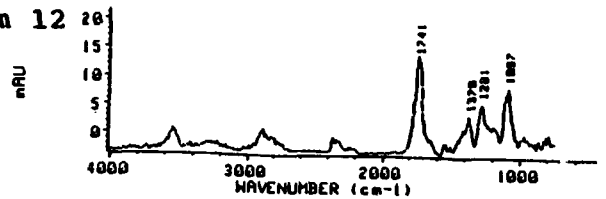

Spectrum 13

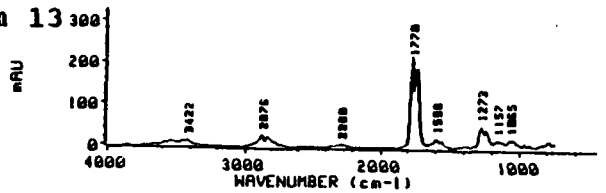

Spectrum 14

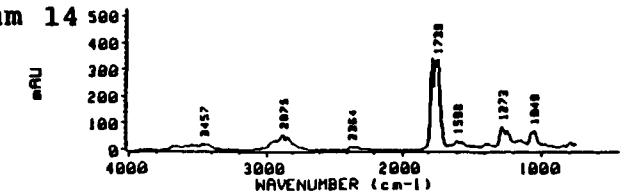

Spectrum 15

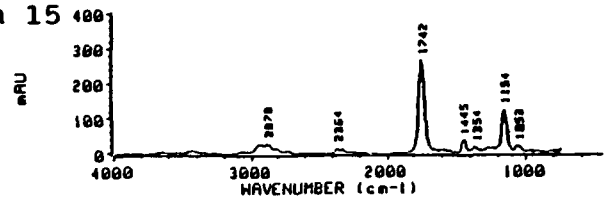

Spectrum 16

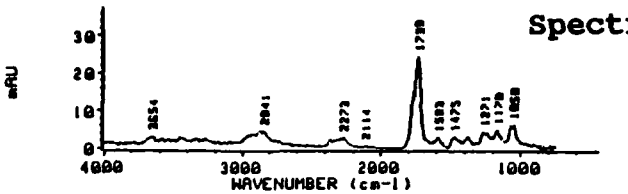

Spectrum 17

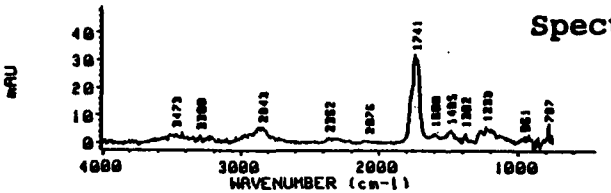

Spectrum 18

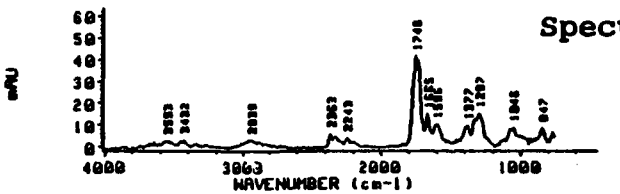

Spectrum 19

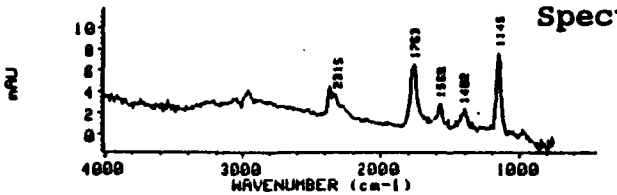

Spectrum 20

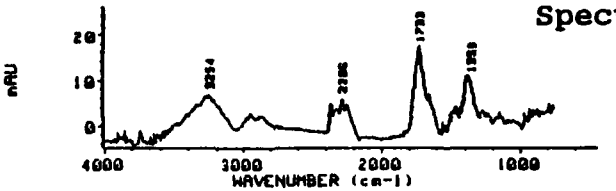

Spectrum 21

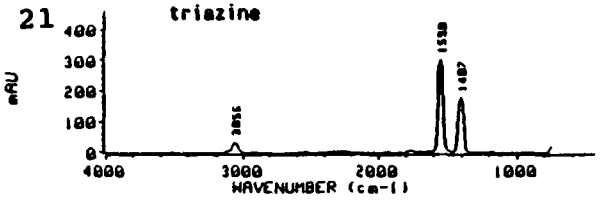

Spectrum 22

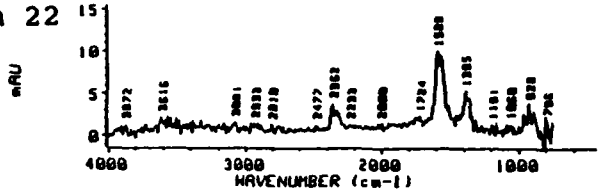

Spectrum 23

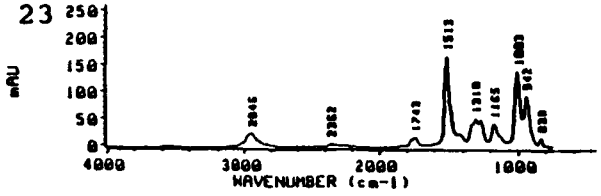

Spectrum 24

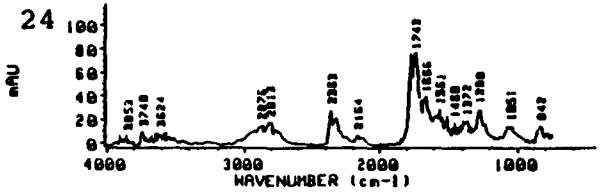

Spectrum 25

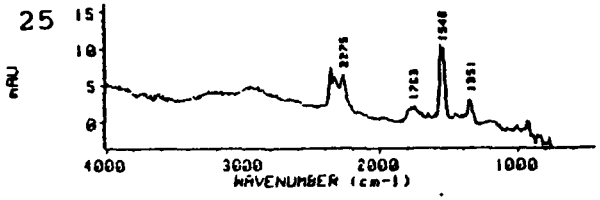

Spectrum 26

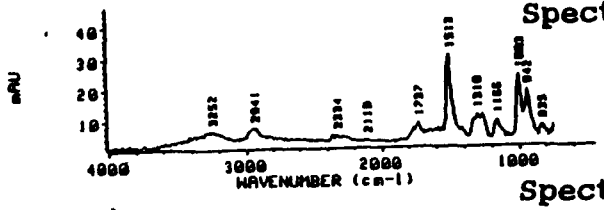

Spectrum 27

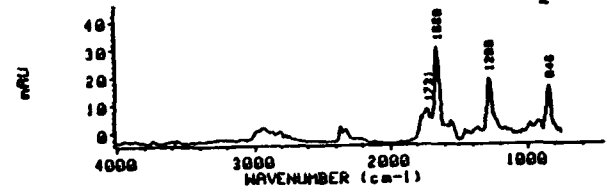

Spectrum 28

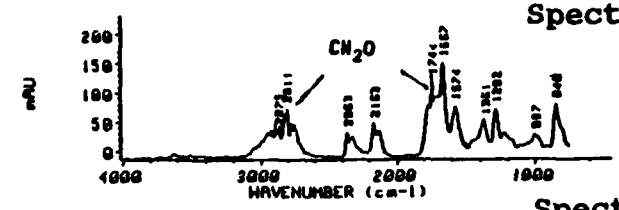

Spectrum 29

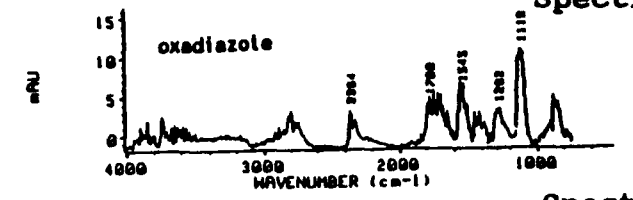

Spectrum 30

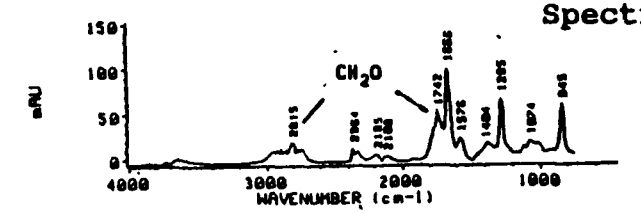

Spectrum 31

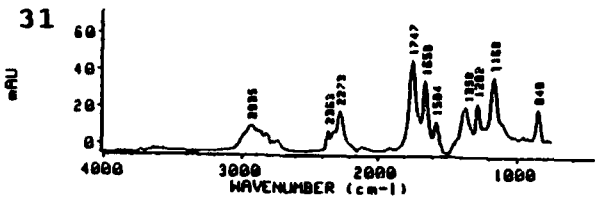

Spectrum 32

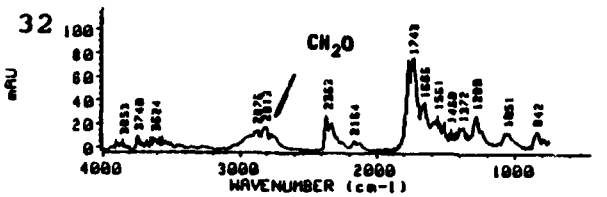

Spectrum 33

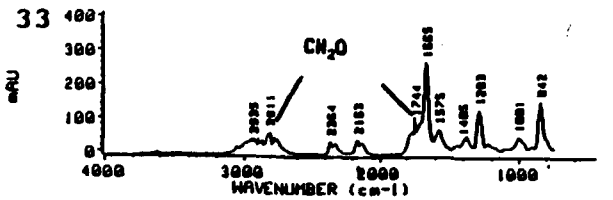

Spectrum 34

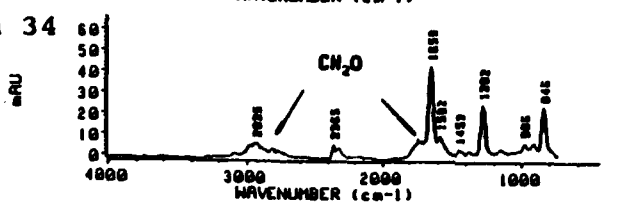

Spectrum 35

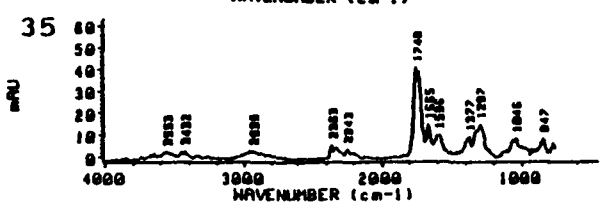

Spectrum 36 is typical of the isocyanates produced by this propellant series. In many cases, the RNCO band overlaps with other bands, in this case with formic acid. Identification of the compound is further complicated by the spectral similarities of different isocyanates. The three model isocyanate spectra below illustrate this point.

Spectrum 36

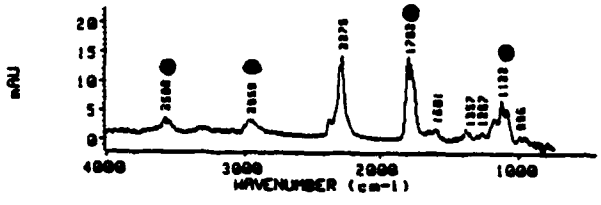

● formic acid bands

three model isocyanate spectra

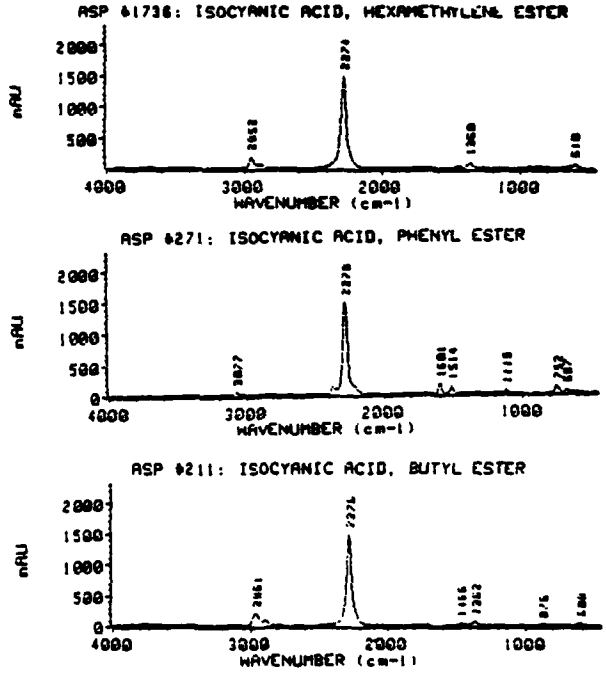

Table A-1. Summary of Samples Having Carbonyl Pyrolysis Spectra Presented in the Appendix

Spectrum No.	Identity	Sample No.	Pyrolysis Temp (°C)	Retention Time (min)
1	Unknown	RDX	400/500	2.8
		19		3.5
		14		11.5
		17		11.0
		20		11.0
		22		11.5
		23		13.5
		24		11.3
		RDX	1,000	3.0
		HMX		11.5
		4		14.5
		14		12.0
		16		12.8
		17		7.5
		19		16.5
		20		8.0
		24		8.4
2	Unknown	RDX	400/500	3.4
		25	1,000	14.7
3	Unknown	RDX	400/500	3.6
		14		12.3
		16		9.0
		RDX	1,000	3.7
		GAP		11.7
		19		4.5
		23		14.7
4	Unknown	RDX	400/500	4.5
		16		4.6
		RDX	1,000	4.2
		15		2.5
		17		6.3

Table A-1. Summary of Samples Having Carbonyl Pyrolysis Spectra Presented in the Appendix (continued)

Spectrum No.	Identity	Sample No.	Pyrolysis Temp (°C)	Retention Time (min)
5	Unknown	RDX 25 20	400/500 1,000	5.4 8.3 9.5
6	Unknown	RDX HMX 25	400/500 1,000	5.6 14.6 13.7
7	Unknown	RDX 22 24	400/500 1,000	6.8 9.0 10.4
8	Unknown	RDX	400/500	8.0
9	Unknown	RDX 9 14 22	400/500	8.7 9.4, 13.0 6.0 10.0
10	Acetamide?	GAP 17 20 21 22 23	1,000	12.1 8.4 9.0 8.5 8.6 8.8
11	Unknown	20 22 23	1,000	15.3 13.0 13.1
12	Triacetin?	4 15 16 18	400/500	6.0, 9.5 10.4 11.5 8.4

Table A-1. Summary of Samples Having Carbonyl Pyrolysis Spectra Presented in the Appendix (continued)

Spectrum No.	Identity	Sample No.	Pyrolysis Temp (°C)	Retention Time (min)
12	Triacetin?	18	1,000	13.0
		23		13.0
		24		12.6
13	Unknown	8	400/500	4.7
		9	1,000	10.0
14	Unknown	17	400/500	12.3
		16		5.9
		21	1,000	7.5
		22		8.0
		23		8.1
		24		7.3
15	Unknown	16	400/500	6.9
		9	1,000	12.5
		16		1.4
16	Unknown	15	400/500	12.6
		20		12.1
		21	1,000	9.5, 14.7
		23		9.6, 12.2
17	Unknown	21	400/500	10.8, 12.0
		9	1,000	9.5
		21		10.5
18	Unknown	HMX	1,000	20.3
		17		13.0
		18		8.0
		21		13.3
		24		8.1, 17.4
19	Unknown	17	1,000	14.2
		18		11.0
		20		10.5
		23		10.2

Table A-2. Summary of Spectra of Carbonyl Pyrolysis Products for Propellant Samples

Sample No.	Low Temperature Pyrolysis Spectra	High Temperature Pyrolysis Spectra
4	12	1
8	13	20
9	9	13, 15, 20
14	1, 2, 9	1
15	12, 16	4
16	2, 4, 12, 14, 15	1, 15
17	1, 14	1, 4, 10, 18, 19
18	12	12, 18, 19
19	1	1, 2
20	1, 16	1, 5, 11, 19
21	17	10, 14, 16, 17, 18
22	1, 9	7, 11, 14
23	1	2, 9, 11, 12, 14, 16, 19
24	1	1, 7, 12, 14, 18
25	5	6
RDX	1, 2, 3, 4, 5, 6, 7, 8, 9	1, 2, 3, 4
HMX	–	1, 6, 18
GAP	–	2, 10
HTPB	–	–

Table A-3. Summary of Spectra of Nitro (RNO_2) Pyrolysis Products for Propellant Samples

Spectrum No.	Identity	Sample No.	Pyrolysis Temperature (°C)	Retention Time (min)
22	Nitromethane	RDX	400/500	6.0
		9		4.0
		14		5.0
		18		5.0
		22		5.0
		24		4.5
		18	1,000	5.0
23	Nitroformamine?	9	400/500	13.5
		14		16.5
		16		8.0
		17		16.5
		8	1,000	10.5
		17		10.5
		20		11.5
		21		10.5
		23		11.5
24	Unknown	RDX	400/500	1.0
		RDX	1,000	1.0
		16		3.5
25	Unknown	18	1,000	8.5

Table A-4. Summary of Spectra of Nitrate (RNO_3) Pyrolysis Products for Propellant Samples

Spectrum No.	Identity	Sample No.	Pyrolysis Temperature (°C)	Retention Time (min)
27	Unknown	4	400/500	7.5
28	Unknown	4	400/500	11.9
30	Unknown	19	400/500	5.2
31	Unknown	19	400/500	5.9
32	Unknown	24	400/500	12.5
33	Unknown	25	400/500	4.0
34	Unknown	25	400/500	5.5

INTENTIONALLY LEFT BLANK.

LIST OF ABBREVIATIONS

BAMO/AMMO	3,3-bis(azidomethyl)oxetane/3-azidomethyl-3-methyl oxetane copolymer
BAMO/THF	3,3-bis(azidomethyl)oxetane/tetrahydrofuran copolymer
BTTN	1,2,4-butane trinitrate
GAP	glycidyl azide polymer
GC	gas chromatography
HMX	cyclotetramethylenetetranitramine
HTPB	hydroxy-terminated polybutadiene
I_{sp}	specific impulse
LOVA	low vulnerability ammunition
MCT	mercury-cadmium-telluride (infrared detector)
m/z	mass to charge ratio (in mass spectrometry)
N-100	trade designation for a polyfunctional isocyanate, manufactured by Mobay
NWC	Naval Weapons Center
P-GC-FTIR	pyrolysis-gas chromatography-Fourier transform infrared
RDX	cyclotrimethylenetrinitramine
TMETN	trimethlyolethane trinitrate

Pyrolysis product notation (used in Tables 3 through 6):

C=O	compound containing a carbonyl functional group (includes aldehydes, amides, and ketones)
PG	permanent gases (includes CH_4, CH_2O, CO, CO_2, NO, and N_2O)
RCH=NH	compound containing an imine functional group
RCOOH	compound containing a carboxylic acid functional group
RNCO	compound containing an isocyanate functional group

RNO_3	compound containing a nitrate functional group
RNO_2	compound containing a nitro functional group

No. of Copies	Organization
2	Administrator Defense Technical Info Center ATTN: DTIC-DDA Cameron Station Alexandria, VA 22304-6145
1	Commander U.S. Army Materiel Command ATTN: AMCDRA-ST 5001 Eisenhower Avenue Alexandria, VA 22333-0001
1	Commander U.S. Army Laboratory Command ATTN: AMSLC-DL 2800 Powder Mill Road Adelphi, MD 20783-1145
2	Commander U.S. Army Armament Research, Development, and Engineering Center ATTN: SMCAR-IMI-I Picatinny Arsenal, NJ 07806-5000
2	Commander U.S. Army Armament Research, Development, and Engineering Center ATTN: SMCAR-TDC Picatinny Arsenal, NJ 07806-5000
1	Director Benet Weapons Laboratory U.S. Army Armament Research, Development, and Engineering Center ATTN: SMCAR-CCB-TL Watervliet, NY 12189-4050
(Unclass. only)1	Commander U.S. Army Armament, Munitions and Chemical Command ATTN: AMSMC-IMF-L Rock Island, IL 61299-5000
1	Director U.S. Army Aviation Research and Technology Activity ATTN: SAVRT-R (Library) M/S 219-3 Ames Research Center Moffett Field, CA 94035-1000

No. of Copies	Organization
1	Commander U.S. Army Missile Command ATTN: AMSMI-RD-CS-R (DOC) Redstone Arsenal, AL 35898-5010
1	Commander U.S. Army Tank-Automotive Command ATTN: ASQNC-TAC-DIT (Technical Information Center) Warren, MI 48397-5000
1	Director U.S. Army TRADOC Analysis Command ATTN: ATRC-WSR White Sands Missile Range, NM 88002-5502
1	Commandant U.S. Army Field Artillery School ATTN: ATSF-CSI Ft. Sill, OK 73503-5000
(Class. only)1	Commandant U.S. Army Infantry School ATTN: ATSH-CD (Security Mgr.) Fort Benning, GA 31905-5660
(Unclass. only)1	Commandant U.S. Army Infantry School ATTN: ATSH-CD-CSO-OR Fort Benning, GA 31905-5660
1	Air Force Armament Laboratory ATTN: WL/MNOI Eglin AFB, FL 32542-5000
	Aberdeen Proving Ground
2	Dir, USAMSAA ATTN: AMXSY-D AMXSY-MP, H. Cohen
1	Cdr, USATECOM ATTN: AMSTE-TC
3	Cdr, CRDEC, AMCCOM ATTN: SMCCR-RSP-A SMCCR-MU SMCCR-MSI
1	Dir, VLAMO ATTN: AMSLC-VL-D
10	Dir, BRL ATTN: SLCBR-DD-T

No. of Copies | Organization

1 HQDA (SARD-TR, C.H. Church)
WASH DC 20310-0103

4 Commander
US Army Research Office
ATTN: R. Ghirardelli
D. Mann
R. Singleton
R. Shaw
P.O. Box 12211
Research Triangle Park, NC
27709-2211

2 Commander
US Army Armament Research,
Development, and Engineering Center
ATTN: SMCAR-AEE-B, D.S. Downs
SMCAR-AEE, J.A. Lannon
Picatinny Arsenal, NJ 07806-5000

1 Commander
US Army Armament Research,
Development, and Engineering Center
ATTN: SMCAR-AEE-BR, L. Harris
Picatinny Arsenal, NJ 07806-5000

2 Commander
US Army Missile Command
ATTN: AMSMI-RD-PR-E, A.R. Maykut
AMSMI-RD-PR-P, R. Betts
Redstone Arsenal, AL 35898-5249

1 Office of Naval Research
Department of the Navy
ATTN: R.S. Miller, Code 432
800 N. Quincy Street
Arlington, VA 22217

1 Commander
Naval Air Systems Command
ATTN: J. Ramnarace, AIR-54111C
Washington, DC 20360

1 Commander
Naval Surface Warfare Center
ATTN: J.L. East, Jr., G-23
Dahlgren, VA 22448-5000

No. of Copies | Organization

2 Commander
Naval Surface Warfare Center
ATTN: R. Bernecker, R-13
G.B. Wilmot, R-16
Silver Spring, MD 20903-5000

5 Commander
Naval Research Laboratory
ATTN: M.C. Lin
J. McDonald
E. Oran
J. Shnur
R.J. Doyle, Code 6110
Washington, DC 20375

1 Commanding Officer
Naval Underwater Systems
Center Weapons Dept.
ATTN: R.S. Lazar/Code 36301
Newport, RI 02840

2 Commander
Naval Weapons Center
ATTN: T. Boggs, Code 388
T. Parr, Code 3895
China Lake, CA 93555-6001

1 Superintendent
Naval Postgraduate School
Dept. of Aeronautics
ATTN: D.W. Netzer
Monterey, CA 93940

3 AL/LSCF
ATTN: R. Corley
R. Geisler
J. Levine
Edwards AFB, CA 93523-5000

1 AL/MKPB
ATTN: B. Goshgarian
Edwards AFB, CA 93523-5000

1 AFOSR
ATTN: J.M. Tishkoff
Bolling Air Force Base
Washington, DC 20332

1 OSD/SDIO/IST
ATTN: L. Caveny
Pentagon
Washington, DC 20301-7100

No. of Copies | Organization

1 Commandant
USAFAS
ATTN: ATSF-TSM-CN
Fort Sill, OK 73503-5600

1 F.J. Seiler
ATTN: S.A. Shackleford
USAF Academy, CO 80840-6528

1 University of Dayton Research Institute
ATTN: D. Campbell
AL/PAP
Edwards AFB, CA 93523

1 NASA
Langley Research Center
Langley Station
ATTN: G.B. Northam/MS 168
Hampton, VA 23365

4 National Bureau of Standards
ATTN: J. Hastie
M. Jacox
T. Kashiwagi
H. Semerjian
US Department of Commerce
Washington, DC 20234

1 Aerojet Solid Propulsion Co.
ATTN: P. Micheli
Sacramento, GA 95813

1 Applied Combustion Technology, Inc.
ATTN: A.M. Varney
P.O. Box 607885
Orlando, FL 32860

2 Applied Mechanics Reviews
The American Society of
Mechanical Engineers
ATTN: R.E. White
A.B. Wenzel
345 E. 47th Street
New York, NY 10017

1 Atlantic Research Corp.
ATTN: M.K. King
5390 Cherokee Avenue
Alexandria, VA 22314

No. of Copies | Organization

1 Atlantic Research Corp.
ATTN: R.H.W. Waesche
7511 Wellington Road
Gainesville, VA 22065

1 AVCO Everett Research
Laboratory Division
ATTN: D. Stickler
2385 Revere Beach Parkway
Everett, MA 02149

1 Battelle
ATTN: TACTEC Library, J. Huggins
505 King Avenue
Columbus, OH 43201-2693

1 Cohen Professional Services
ATTN: N.S. Cohen
141 Channing Street
Redlands, CA 92373

1 Exxon Research & Eng. Co.
ATTN: A. Dean
Route 22E
Annandale, NJ 08801

1 Ford Aerospace and
Communications Corp.
DIVAD Division
Div. Hq., Irvine
ATTN: D. Williams
Main Street & Ford Road
Newport Beach, CA 92663

1 General Applied Science
Laboratories, Inc.
77 Raynor Avenue
Ronkonkama, NY 11779-6649

1 General Electric Ordnance
Systems
ATTN: J. Mandzy
100 Plastics Avenue
Pittsfield, MA 01203

1 General Motors Rsch Labs
Physical Chemistry Department
ATTN: T. Sloane
Warren, MI 48090-9055

No. of Copies | Organization

2 Hercules, Inc.
Allegheny Ballistics Lab.
ATTN: W.B. Walkup
E.A. Yount
P.O. Box 210
Rocket Center, WV 26726

1 Alliant Techsystems, Inc.
Marine Systems Group
ATTN: D.E. Broden/
MS MN50-2000
600 2nd Street NE
Hopkins, MN 55343

1 Alliant Techsystems, Inc.
ATTN: R.E. Tompkins
MN38-3300
5700 Smetana Drive
Minnetonka, MN 55343

1 IBM Corporation
ATTN: A.C. Tam
Research Division
5600 Cottle Road
San Jose, CA 95193

1 IIT Research Institute
ATTN: R.F. Remaly
10 West 35th Street
Chicago, IL 60616

2 Director
Lawrence Livermore
National Laboratory
ATTN: C. Westbrook
M. Costantino
P.O. Box 808
Livermore, CA 94550

1 Lockheed Missiles & Space Co.
ATTN: George Lo
3251 Hanover Street
Dept. 52-35/B204/2
Palo Alto, CA 94304

1 Director
Los Alamos National Lab
ATTN: B. Nichols, T7, MS-B284
P.O. Box 1663
Los Alamos, NM 87545

No. of Copies | Organization

1 National Science Foundation
ATTN: A.B. Harvey
Washington, DC 20550

1 Olin Ordnance
ATTN: V. McDonald, Library
P.O. Box 222
St. Marks, FL 32355-0222

1 Paul Gough Associates, Inc.
ATTN: P.S. Gough
1048 South Street
Portsmouth, NH 03801-5423

2 Princeton Combustion
Research Laboratories, Inc.
ATTN: M. Summerfield
N.A. Messina
475 US Highway One
Monmouth Junction, NJ 08852

1 Hughes Aircraft Company
ATTN: T.E. Ward
8433 Fallbrook Avenue
Canoga Park, CA 91303

1 Rockwell International Corp.
Rocketdyne Division
ATTN: J.E. Flanagan/HB02
6633 Canoga Avenue
Canoga Park, CA 91304

4 Director
Sandia National Laboratories
Division 8354
ATTN: R. Cattolica
S. Johnston
P. Mattern
D. Stephenson
Livermore, CA 94550

1 Science Applications, Inc.
ATTN: R.B. Edelman
23146 Cumorah Crest
Woodland Hills, CA 91364

3 SRI International
ATTN: G. Smith
D. Crosley
D. Golden
333 Ravenswood Avenue
Menlo Park, CA 94025

No. of Copies — Organization

1 Stevens Institute of Tech.
Davidson Laboratory
ATTN: R. McAlevy, III
Hoboken, NJ 07030

1 Sverdrup Technology, Inc.
LERC Group
ATTN: R.J. Locke, MS SVR-2
2001 Aerospace Parkway
Brook Park, OH 44142

1 Sverdrup Technology, Inc.
ATTN: J. Deur
2001 Aerospace Parkway
Brook Park, OH 44142

1 Thiokol Corporation
Elkton Division
ATTN: S.F. Palopoli
P.O. Box 241
Elkton, MD 21921

3 Thiokol Corporation
Wasatch Division
ATTN: S.J. Bennett
P.O. Box 524
Brigham City, UT 84302

1 United Technologies Research Center
ATTN: A.C. Eckbreth
East Hartford, CT 06108

3 United Technologies Corp.
Chemical Systems Division
ATTN: R.S. Brown
T.D. Myers (2 copies)
P.O. Box 49028
San Jose, CA 95161-9028

1 Universal Propulsion Company
ATTN: H.J. McSpadden
Black Canyon Stage 1
Box 1140
Phoenix, AZ 85029

1 Veritay Technology, Inc.
ATTN: E.B. Fisher
4845 Millersport Highway
P.O. Box 305
East Amherst, NY 14051-0305

No. of Copies — Organization

1 Brigham Young University
Dept. of Chemical Engineering
ATTN: M.W. Beckstead
Provo, UT 84058

1 California Institute of Tech.
Jet Propulsion Laboratory
ATTN: L. Strand/MS 512/102
4800 Oak Grove Drive
Pasadena, CA 91109

1 California Institute of Technology
ATTN: F.E.C. Culick/
MC 301-46
204 Karman Lab.
Pasadena, CA 91125

1 University of California
Los Alamos Scientific Lab.
P.O. Box 1663, Mail Stop B216
Los Alamos, NM 87545

1 University of California, Berkeley
Chemistry Deparment
ATTN: C. Bradley Moore
211 Lewis Hall
Berkeley, CA 94720

1 University of California, San Diego
ATTN: F.A. Williams
AMES, B010
La Jolla, CA 92093

2 University of California, Santa Barbara
Quantum Institute
ATTN: K. Schofield
M. Steinberg
Santa Barbara, CA 93106

1 University of Colorado at Boulder
Engineering Center
ATTN: J. Daily
Campus Box 427
Boulder, CO 80309-0427

No. of Copies | Organization

2 University of Southern California
Dept. of Chemistry
ATTN: S. Benson
C. Wittig
Los Angeles, CA 90007

1 Cornell University
Department of Chemistry
ATTN: T.A. Cool
Baker Laboratory
Ithaca, NY 14853

1 University of Delaware
ATTN: T. Brill
Chemistry Department
Newark, DE 19711

1 University of Florida
Dept. of Chemistry
ATTN: J. Winefordner
Gainesville, FL 32611

3 Georgia Institute of Technology
School of Aerospace Engineering
ATTN: E. Price
W.C. Strahle
B.T. Zinn
Atlanta, GA 30332

1 University of Illinois
Dept. of Mech. Eng.
ATTN: H. Krier
144MEB, 1206 W. Green St.
Urbana, IL 61801

1 Johns Hopkins University/APL
Chemical Propulsion
Information Agency
ATTN: T.W. Christian
Johns Hopkins Road
Laurel, MD 20707

1 University of Michigan
Gas Dynamics Lab
Aerospace Engineering Bldg.
ATTN: G.M. Faeth
Ann Arbor, MI 48109-2140

No. of Copies | Organization

1 University of Minnesota
Dept. of Mechanical
Engineering
ATTN: E. Fletcher
Minneapolis, MN 55455

3 Pennsylvania State University
Applied Research Laboratory
ATTN: K.K. Kuo
H. Palmer
M. Micci
University Park, PA 16802

1 Pennsylvania State University
Dept. of Mechanical Engineering
ATTN: V. Yang
University Park, PA 16802

1 Polytechnic Institute of NY
Graduate Center
ATTN: S. Lederman
Route 110
Farmingdale, NY 11735

2 Princeton University
Forrestal Campus Library
ATTN: K. Brezinsky
I. Glassman
P.O. Box 710
Princeton, NJ 08540

1 Purdue University
School of Aeronautics
and Astronautics
ATTN: J.R. Osborn
Grissom Hall
West Lafayette, IN 47906

1 Purdue University
Department of Chemistry
ATTN: E. Grant
West Lafayette, IN 47906

2 Purdue University
School of Mechanical
Engineering
ATTN: N.M. Laurendeau
S.N.B. Murthy
TSPC Chaffee Hall
West Lafayette, IN 47906

No. of
Copies Organization

1 Rensselaer Polytechnic Inst.
Dept. of Chemical Engineering
ATTN: A. Fontijn
Troy, NY 12181

1 Stanford University
Dept. of Mechanical
Engineering
ATTN: R. Hanson
Stanford, CA 94305

1 University of Texas
Dept. of Chemistry
ATTN: W. Gardiner
Austin, TX 78712

1 University of Utah
Dept. of Chemical Engineering
ATTN: G. Flandro
Salt Lake City, UT 84112

1 Virginia Polytechnic
Institute and
State University
ATTN: J.A. Schetz
Blacksburg, VA 24061

1 Freedman Associates
ATTN: E. Freedman
2411 Diana Road
Baltimore, MD 21209-1525

INTENTIONALLY LEFT BLANK.

USER EVALUATION SHEET/CHANGE OF ADDRESS

This laboratory undertakes a continuing effort to improve the quality of the reports it publishes. Your comments/answers below will aid us in our efforts.

1. Does this report satisfy a need? (Comment on purpose, related project, or other area of interest for which the report will be used.) _____

2. How, specifically, is the report being used? (Information source, design data, procedure, source of ideas, etc.) _____

3. Has the information in this report led to any quantitative savings as far as man-hours or dollars saved, operating costs avoided, or efficiencies achieved, etc? If so, please elaborate. _____

4. General Comments. What do you think should be changed to improve future reports? (Indicate changes to organization, technical content, format, etc.) _____

BRL Report Number BRL-TR-3288 Division Symbol _____

Check here if desire to be removed from distribution list. ____

Check here for address change. ____

Current address: Organization _____
Address _____

DEPARTMENT OF THE ARMY
Director
U.S. Army Ballistic Research Laboratory
ATTN: SLCBR-DD-T
Aberdeen Proving Ground, MD 21005-5066

OFFICIAL BUSINESS

BUSINESS REPLY MAIL
FIRST CLASS PERMIT No 0001, APG, MD

Postage will be paid by addressee.

NO POSTAGE NECESSARY IF MAILED IN THE UNITED STATES

Director
U.S. Army Ballistic Research Laboratory
ATTN: SLCBR-DD-T
Aberdeen Proving Ground, MD 21005-5066